EVALUATION OF TITANIA-BASED THIN FILMS FABRICATED VIA THE AQUEOUS SPRAY METHOD FOR APPLICATIONS AS ANTI-SOILING COATINGS ON SOLAR CELL COVER GLASS

A THESIS SUBMITTED IN PARTIAL FULFILMENT OF THE

REQUIREMENTS FOR THE DEGREE OF

MASTER OF SCIENCE IN RENEWABLE ENERGY

OF

THE UNIVERSITY OF NAMIBIA

BY

KLAUDIA NDAWAPEKA MWATILE

218201499

APRIL 2025

SUPERVISOR: DR. PHILIPUS N. HISHIMONE, UNIVERSITY OF NAMIBIA

Abstract

The growing demand for sustainable energy has made solar energy essential in the world energy transition. To maximize power output, solar PV systems must operate effectively. However, factors like soiling on the solar cell cover can reduce efficiency and overall power output. Traditional cleaning methods are typically expensive and labor-intensive, therefore emphasizing the need for simpler, cost-effective solutions like anti-soiling coatings. This study investigates the structural, optical, and photocatalytic properties of aluminum (Al), zinc (Zn), and copper (Cu) doped titanium dioxide (TiO_2) thin films prepared via an aqueous spray method. Aqueous precursor solutions were formulated by mixing Ti^{4+} complexes with Al^{3+}, Zn^{2+}, or Cu^{2+} complexes, with molar percentages varying from 0% to 10%. The results from UV-vis spectroscopy indicated that doping significantly enhanced the optical properties of TiO_2 thin films, with Al, Zn, and Cu-doped films showing higher transmittance than undoped TiO_2. X-ray diffraction (XRD) confirmed that all samples retained the anatase phase of TiO_2 without secondary phases of the dopants. Photocatalytic degradation tests revealed that 6% Cu-doped TiO_2 exhibited the highest degradation rate of 28% for methyl orange (MO), while 8% Al-doped and 2% Zn-doped films showed optimal activity at their respective levels. These findings suggest that doping TiO_2 thin films at appropriate doping concentrations can enhance their optical properties and photocatalytic efficiency, making them promising candidates for anti-soiling applications on solar cell covers.

Keywords: Thin films, TiO_2, Aqueous spray method, doping

List of Publication(s)/Conference(s) Proceedings

Klaudia N. Mwatile, Haitange Hamwaama, Gaby K. Mutenda, Tunelago Kadhingula, and Philipus N. Hishimone. Characterization of aluminium and zinc-doped TiO_2 thin films fabricated by the aqueous spray method. 5-6 September 2024, The 29th International SPACC Symposium, Hokkaido University, Sapporo, Japan

Table of Contents

Abstract i

List of Publication(s)/Conference(s) Proceedings ii

List of figures vi

List of abbreviations and Acronyms viii

Acknowledgments x

Dedication xi

Declaration xii

CHAPTER 1 1

Introduction 1

1.1 Background 1

1.2 Statement of the problem 2

1.3 Objectives of the study 2

1.4 Significance of the study 2

1.5 Limitations of the study 2

1.6 Delimitations of the study 3

CHAPTER 2 4

Literature Review 4

2.1 Soiling effect on solar cell performance 4

2.2 Titanium dioxide (TiO_2) and its properties 9

2.3 Applications of TiO_2 11

2.4 TiO_2 as an anti-soiling coating 16

2.5 Effect of doping on TiO_2 19

2.6 Established methods for the fabrication of thin films 20

2.7 TiO_2-based thin films fabricated by the aqueous spray method. 22

CHAPTER 3 24

Materials and Methods 24

3.1 Chemicals 24

3.2 Preparation of ammonium titanyl oxalate monohydrate $(NH_4)_2[Ti(C_2O_4)_2O]\cdot H_2O$ (Ti^{4+} complex) 24

3.3 Preparation of undoped Ti^{4+} precursor solution 25

3.4 Preparation of Al^{3+}, Zn^{2+} and Cu^{2+} precursor solutions 25

3.5 Preparation of Al, Zn and Cu-doped Ti^{4+} precursor solutions 25

3.6 Fabrication of TiO_2-based thin films 26

3.7 Heat-treatment 27

3.8 Characterisation 28

3.9 Photocatalytic Activity of the TiO_2 thin films 28

CHAPTER 4 30

Results and Discussion 30

4.1 Prepared precursor solutions and resultant thin films 30

4.2 Characterisation of the synthesized $(NH_4)_2[Ti(C_2O_4)_2O]\cdot H_2O$ 31

4.2 Crystal Structures 32

4.3. Optical properties 35

4.4 Photocatalytic activity 40

CHAPTER 5 48

Conclusion 48

CHAPTER 6 49

Recommendations 49

APPENDIX I: Ethical clearance 67

Appendix II Research permission letter 68

List of figures

Figure 2.1. Illustration of soiling on solar cell cover glass 5

Figure 2.2 Manual cleaning of solar cells at the University of Namibia 6

Figure 2.3 Classification of Surface wettability based on Contact Angle**.** [27] 8

Figure 2.4 Schematic representation of the self-cleaning mechanism by degradation of organic contaminants. 17

Figure 3.1 Illustration of spray-coating set-up 27

Figure 4.1 Precursor solutions contain (a) Ti^{4+} (b) Al^{3+} (c) Zn^{2+} and (d) Cu^{2+} ions 30

Figure 4.2 (a) Al-doped Ti^{4+} precursor solutions, **(b)** Zn-doped Ti^{4+} precursor solutions and **(c)** Cu-doped Ti^{4+} precursor solutions 30

Figure 4.3 Fabricated thin thins..... 31

Figure 4.4 FTIR spectra of ammonium oxalate, oxalic acid and ammonium titanyl oxalate monohydrate..... 32

Figure 4.5 XRD diffractogram of undoped and Al-doped TiO_2 thin films 33

Figure 4.6 XRD diffractogram for undoped and Zn-doped TiO2 thin films..... 34

Figure 4.7 XRD diffractogram for undoped and Zn-doped TiO2 thin films..... 35

Figure 4.8 UV-vis transmittance spectra of Al-doped TiO_2 thin films at different doping concentrations. 36

Figure 4.9 UV-vis transmittance spectra of Zn-doped TiO_2 thin films at different doping concentrations 38

Figure 4.10 UV-vis transmittance spectra of Cu-TiO_2 thin films at different doping concentrations 39

Figure 4.11 MO orange absorbance spectra before and after photocatalysis in the presence of undoped and Al-doped TiO_2 41

Figure 4.12 MO orange absorbance spectra before and after photocatalysis in the presence of undoped and Zn-doped TiO_2 43

Figure 4.13 MO orange absorbance spectra before and after photocatalysis in the presence of undoped and Cu-doped TiO_2 44

Figure 4.14 Degradation efficiency of undoped and Al-doped TiO_2 thin films on MO. 45

Figure 4.15 Degradation efficiency of undoped and Zn-doped TiO_2 thin films on MO 46

Figure 4.16 Degradation efficiency of undoped and Cu-doped TiO_2 thin films on MO 47

List of abbreviations and Acronyms

Ag	Silver
Al	Aluminium
CNTs	Carbon nanotubes
CVD	Chemical vapor deposition
CSP	Concentrated solar power
DOS	Density of states
FT-IR	Fourier Transform Infrared Spectroscopy
HCl	Hydrochloric acid
H_2	Hydrogen
MB	Methyl blue
MO	Methyl orange
Mn	Manganese
N	Nitrogen
Ni	Nickel
O_2•	Superoxide radicals

OH^-	Hydroxyl groups
OH•	Hydroxyl radicals
PLD	Pulsed laser deposition
Pt	Platinum
KI	Potassium iodide
SEM	Scanning Electron Microscope
TiO_2	Titanium dioxide
TTIP	Titanium Tetraisopropoxide
V	Vanadium
UV-Vis	Ultra-violet Visible
XRD	X-ray Diffraction
Zn	Zinc

Acknowledgments

- First and foremost, I would like to acknowledge God almighty for the strength and guidance he has provided me with through this journey.
- I extend my deepest appreciation to my supervisor Dr Philipus Hishimone for his invaluable guidance, support, leadership and encouragement. Your insights and expertise have been instrumental in shaping my research and I am grateful and indebted to you for that.
- I would like to express my gratitude to Professor Hiroki Nagai and the Kokaguin University for their assistance in analysing my samples. This experience provided critical insights that significantly enhanced my research.
- A special thanks goes to my fellow colleagues and friends in the laboratory for their assistance and support during this research process. Your contributions have made a significant difference.
- I would like to acknowledge my family for their unconditional love and support. To my parents, especially my father for instilling in me the values of hard work and perseverance.
- This thesis is a result of collective efforts, and I am truly grateful to everyone who has played a role in this achievement.

Dedication

This thesis is dedicated to my siblings, my parents and to my Lord Jesus, whose love and support have been my foundation throughout this journey. Your sacrifices and your presence have been a source of comfort and motivation.

This work is a testament to your unfailing love and support.

Declaration

I, Klaudia N Mwatile, hereby declare that this study is my own work and is a true reflection of my research, and that this work, or any part thereof has not been submitted for a degree at any other institution. No part of this thesis/dissertation may be reproduced, stored in any retrieval system, or transmitted in any form, or by means (e.g. electronic, mechanical, photocopying, recording or otherwise) without the prior permission of the author, or The University of Namibia in that behalf.

I, Klaudia N Mwatile, grant The University of Namibia the right to reproduce this thesis in whole or in part, in any manner or format, which The University of Namibia may deem fit.

Klaudia N Mwatile		April 2024
Name of Student	Signature	Date

CHAPTER 1 : Introduction

1.1 Background

The use of solar energy has grown to become the basis of the approach to sustainable and renewable power sources [1]. With this regard, solar photovoltaic (PV) systems require effective and efficient operation to achieve maximum power output [2]. This can be achieved by preserving the optical and structural integrity of the solar cell cover glass which protects the underlying photovoltaic layers [2]. Employing scratch-resistant coatings, anti-soiling coatings and routine maintenance including cleaning of the cover glass to ensure optimal light transmission and protection against environmental factors are some of the ways used in the attempt to keep solar photovoltaic systems working efficiently [3]. However, there are associated costs including the need for high-quality materials and the regular cleaning and maintenance of solar panels [3]. While some improvements have been made, the application of anti-soiling coatings has also been hindered by several research concerns, including the optimization of fabrication methods, composition for enhanced anti-soiling performance and uncertainties regarding long-term durability [4].

1.2 Statement of the problem

The need for regular cleaning and maintenance of solar cell cover glass is often labour-intensive and costly. Additionally, current fabrication methods for thin films as anti-soiling coatings are expensive and complicated. Therefore, there is a need for continued, research on simpler and cheaper fabrication methods of these coatings.

1.3 Objectives of the study

The purpose of the study was to evaluate the use TiO_2-based thin films fabricated via the aqueous spray-coating method as anti-soiling coatings for solar cell cover glass.

The specific objectives of this study were to:

a) fabricate TiO_2-based thin films via the aqueous spray method

b) characterize the fabricated thin films

c) evaluate thin films' suitability for anti-soiling coatings

1.4 Significance of the study

The utilization of TiO_2-based thin films in this research not only exhibits their eco-friendly nature but also highlights their cost-effectiveness. The successful development of TiO_2-based anti-soiling coatings for solar cell cover glass could significantly improve the operational efficiency and lifespan of solar panels, making them more reliable and cost-effective.

1.5 Limitations of the study

Thin films fabrication and characterization needed to be done within a short period time from each other. However, equipment such as X-ray diffractometer (XRD) were not available at UNAM therefore samples had to be sent to other institutions. These extended

periods between the fabrication and acquiring of characterization results did not give us ample time to optimize the fabricated thin films or do necessary modifications.

1.6 Delimitations of the study

The study primarily focused on TiO_2-based thin films produced through the aqueous spray method, without investigating alternative materials or fabrication techniques. Moreover, the research was limited to laboratory-based experiments and characterization procedures and the primary application considered for the TiO_2-based thin films was their use as anti-soiling coatings on solar cell cover glass, excluding other potential applications.

CHAPTER 2 : Literature Review

2.1 Soiling effect on solar cell performance

Solar energy is one the sources of renewable energy that has been broadly studied because of its ability to produce power effectively without imposing negative environmental effects [5, 6]. Solar photovoltaic (PV) systems are believed to have a lifespan of about 25 years. However, several factors such as soiling can hinder the efficient operation of the solar cells and overall reduce the power output of the PV systems [7, 8]. Soiling refers to the accumulation of dust and dirt particles on the cover glass of solar cells and is considered one of the significant challenges that reduce the performance and the efficiency of PV systems [9, 10]. This is attributed to the fact that soiling on solar cell cover glass reduces the amount of sunlight that can penetrate the solar cell and therefore less amount of sunlight is transmitted and less energy is converted to power leading to optical losses [11]. Factors that result in soiling include various sources such as wind, humidity and dew amongst many other factors [8]. **Figure 2.1** displays the accumulation of soiling on the solar cell cover glass. In a study by Rahoma et al. a decrease in power output after just one month of dust exposure on solar cells was observed with optical losses reaching 33.5%, escalating to 65.8% after six months without cleaning [12]. In a separate study by Sayigh et al. reduction in transmission up to 65% was observed on dust-covered glass panels after 38 days, with varying effects based on tilt angles [13].

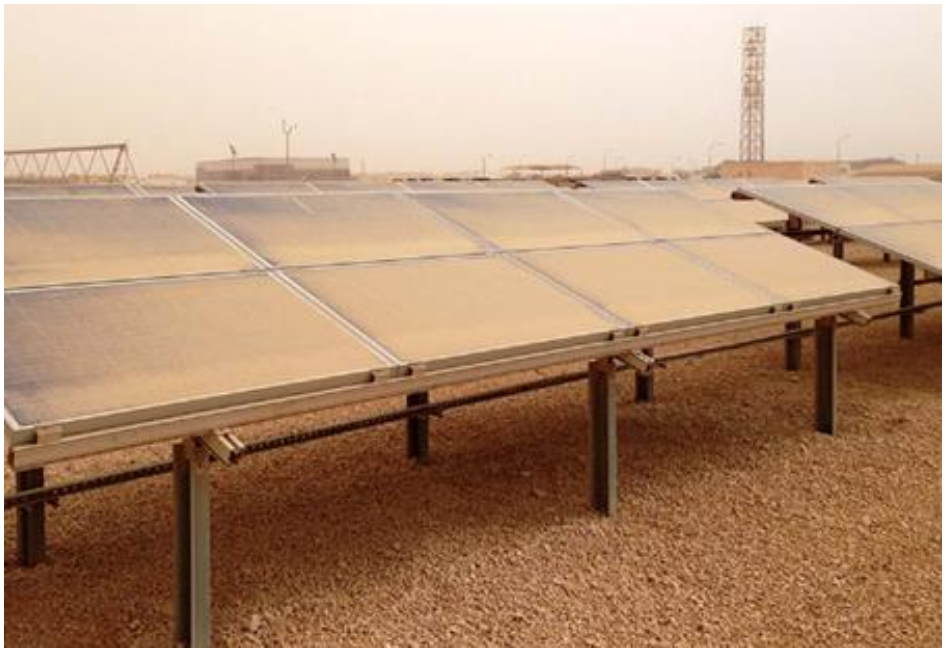

Figure 2.1. Illustration of soiling on solar cell cover glass

Soiling can also lead to partial shading, which may result in the formation of hot spots which cause certain cells to resist the current generated by the other cells, ultimately decreasing energy efficiency and reducing the lifespan of the module [10]. Additionally, it has been reported that the losses that result from soiling do not only affect the power output, but they also results in economic losses whereby a vast amount of money is put into the maintenance and cleaning of the PV modules [14]. It has been noted that fine dust particles are the most likely to reduce the amount of light transmitted by PV modules compared to coarse particles. This is because coarse particles are easily swept away by wind whilst fine particles are not easily swept away and remain settled on the solar cell cover glass [15]. To maintain cleanliness and reduce soiling, various soiling mitigation techniques have been developed. These techniques include but are not limited to manual, natural and mechanical cleaning methods [16]. Manual cleaning methods makes use of soft brushes that have a direct and continuous water supply that splashes along with

cleaning [17]. Coarse cloths or sponges are also used with the help of manual labor to remove dirt and dust that has adhered onto the surface PV modules as shown in **Figure 2.2** [9, 17–19].

Figure 2.2 Manual cleaning of solar cells at the University of Namibia

Although manual cleaning has been one of the first methods used in the cleaning of PV modules, it has found some shortcomings. These shortcomings encompass the need for regular cleaning, high cost involved in the use of water to clean and manual labor which requires skilled personal in addition to repeated rubbing and direct contact of the brushes with the surface of the PV module which can cause damage to the PV modules and reduce the lifespan and efficiency of the PV modules overtime [9, 17]. On the other hand, natural methods of cleaning removes dust with the aid of natural sources such as heavy rainfall, wind and gravity [20]. Although rainfall was found to effectively remove dust from the

surface of PV modules, it also leads to the reduction in the generation of energy as heavy rain can lead to non-uniform cleaning while light rainfall can lead to mud puddles on the surface of the PV modules [21]. Additionally, rainfall is scarce and irregular in arid and semi-arid areas and therefore it becomes unreliable [22]. Wind has been found to remove coarse dust particles that are 1μm in diameter as strong winds with moderate speed do not cause dust. However, fine dust particles cannot be removed by wind as extreme wind velocities are needed for the removal of fine dust particles [9, 17].

Like rainfall, wind becomes unreliable as winds are influenced by seasonal variations and changing weather patterns [21]. Gravity is another natural form of cleaning PV modules as inclined positions of the PV modules as increased tilt angles from 0° to 90° makes it easier for dust particles to be removed with the aid of gravity however these angles minimize the amount of light transmission received by the modules [23]. Mechanical cleaning methods makes use of automated robotic systems that are equipped with signal receivers, position sensors and dust concentration sensors to clean and brush PV modules by wiping, brushing and blowing off dust [9, 24]. This method of cleaning requires less manual labor as the robotic cleaners are independent. However, the use of these systems involve high operational costs, complex mechanical maintenance and the effectiveness of these systems against soiling has not been well established [9, 17]. Additionally, high energy is required to operate these systems as they need power to work which is not cost effective [25].

Anti-soiling coatings which are categorized as self-cleaning coatings, have been integrated into PV module structures as another technique that is used to minimize the accumulation of dust on solar cell cover glasses [26]. These anti-soiling coatings have

hydrophilic and/ or hydrophobic properties where they exhibit wettability behavior resulting in their self-cleaning abilities [26]. Hydrophobic anti-soiling coatings are those that naturally repel water by forming spherical droplets upon contact with water and roll down the surface washing away dirt off the surface. Hydrophilic anti-soling coatings on the other hand naturally attract water forming a droplet that spreads over the area of the surface and sweeps dirt away [18].

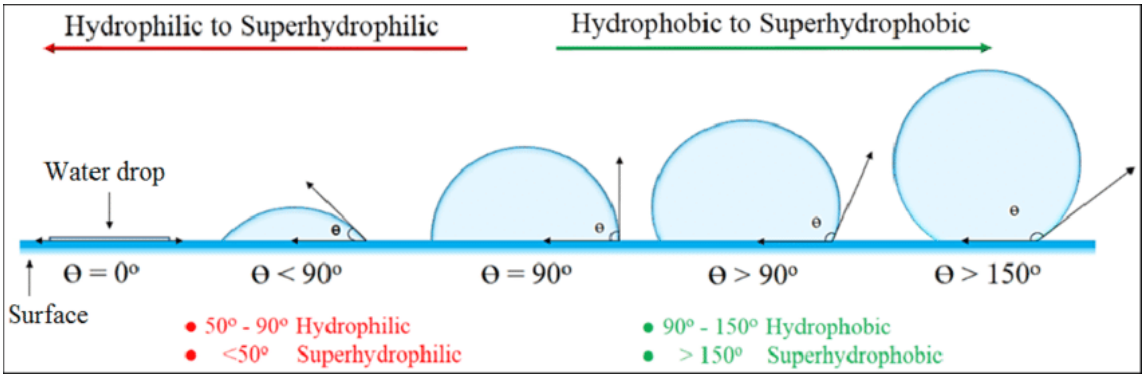

Figure 2.3 Classification of Surface wettability based on Contact Angle**.** [27]

The hydrophobic and hydrophilic nature of anti-soiling coatings is determined by their wettability properties which are measured by the water contact angle (WCA) as shown in figure 2.3. The WCA refers to the angle a liquid form when it comes into contact with a solid surface and this angle is influenced by the adhesion or cohesion properties of both the liquid and the solid [18]. WCA that are below 90° are considered hydrophilic while those that are above are considered to be hydrophobic [28].

Hydrophilic coatings can form WCA of less than 90° because they contain weak cohesive forces and strong adhesive forces therefore liquid molecules are attracted to the solid surfaces which results in the wettability of the surface [18]. In addition, when the WCA is very low such that it reaches 0° it is called super-hydrophilic. On the other hand,

hydrophobic coatings form WCA of more than 90° as the they have strong cohesive forces and weak adhesive forces therefore liquids tend to attract each other more than they attract surfaces, and this results in repulsions and when the WCA reaches about 180° the coating is called super-hydrophobic [18].

2.2 Titanium dioxide (TiO_2) and its properties

Titanium dioxide (TiO_2) which is alternatively referred to as titania owing to its naturally occurring oxide of titanium, is a metal oxide semi-conductor that has been widely studied owing to its chemical stability, non-toxicity, affordability and excellent photocatalytic activity [29, 30]. As a result of its properties, TiO_2 has been employed as a coating in several applications ranging from photovoltaics, photocatalysis, sensors, photo-electronics and electrochemical applications [31].

TiO_2 extensively exits in three crystalline phases namely anatase, rutile and brookite [29] Of the three phases, the anatase and rutile crystalline phases are the most commonly studied phases compared to the brookite phase as they both have practical significance in the structure of TiO_2. For instance, the rutile phase is more thermodynamically stable while the anatase phase exhibits high photocatalytic activity and brookite is the least stable therefore the least studied [32] Both the anatase and rutile phases have a tetragonal shape but they do not belong to the same structural phase while the brookite phase has an orthorhombic shape [33].

Previous studies have indicated that coupling the rutile and anatase phases shifts electrons from the rutile phase to the anatase phase which practically produces great electron-hole pair separation which further increases the photocatalytic activity of the anatase compared

to when only the anatase phase is present [34]. Furthermore, at very high temperatures ranging from about 450-1200℃, the anatase phase can convert to the rutile phase due to its low density [35]. Additionally, the anatase phase also poses a low dielectric constant and high electron mobility which makes it useful in solar cell applications [36].

At wavelengths smaller than 386 nm, anatase absorbs light within the UV range and for this reason it has been useful in the production of paints and paper in contrast to rutile which is more resistant to UV light compared therefore it is mostly used for paints [30].

Given that TiO_2 has applications in electronic devices and solar cells, its optical properties play a very significant role in these applications and these optical properties include its chemical stability, high transparency in the UV region and optical band gap [37]. The optical properties of TiO_2 nanoparticles in particular can be influenced by the particle size whereby reducing the size of TiO_2 nanoparticles below 200nm changes its optical properties from opaque to transparent which makes it accessible in the UV region [38]. Additionally, the anatase crystalline phase of TiO_2 demonstrates good catalytic efficiency and electron mobility which is an advantageous characteristic of TiO_2 for applications in photovoltaic and photocatalytic [39, 40]. The enhanced photoactivity associated with the anatase phase has been attributed to its decreased oxygen adsorption capacity, elevated degrees of hydroxylation, and a marginally elevated Fermi level [39]. Conversely, the rutile phase is distinguished by its elevated refractive index and significant optical absorptivity, which makes it useful in optical communication devices such as modulators, switches, and isolators [40]. The band gap of TiO_2 differs with its phase whereby the anatase phase has a band gap of 3.2 eV and the rutile phase has a band gap of about 3.0 eV. Therefore, in this context, the anatase phase is perceived as the active photocatalytic

entity, a distinction that can be linked to the chemical characteristics of TiO_2 and the formation of electron-hole pairs that stem from its capacity to absorb UV light, which aligns with its band gap [41]

The particle and crystal size of TiO_2 influences its electronic properties[38]. In optoelectronic devices, it has been reported that the anatase phase is more favourable for the production of these devices attributed to the fact that the anatase phase has a smaller electron mass than all the other phases which elevates the mobility of its charge carriers [42]. The electronic properties of TiO_2 can also be altered by introducing dopants of either metals or non-metals to narrow its band gap making it even more responsive to UV light [43].

2.3 Applications of TiO_2

Since TiO_2 is known for its remarkable properties, it has been used in a wide range of applications including nanobiotechnology and nanomedicine, energy devices, energy storage and production, environmental protection as well as industrial production [44].

In nanobiotechnology, TiO_2 has gained attention due to its hydrolysis, oxidative properties as well as antimicrobial properties which also make it non-toxic [45, 46]. A study investigated the photocatalytic impact of TiO_2 nanoparticles on biofilm production by Listeria monocytogenes, finding that UV-activated TiO_2 led to a significant reduction in biofilm mass when deposited on stainless steel and glass surfaces [47]. In a separate study, the addition of potassium iodide (KI) as an inorganic salt enhanced the photocatalytic activity of TiO_2 against fungi and various bacteria, yielding an increase in antimicrobial efficacy, dependent on UV light intensity and TiO_2 concentration [48]. Additionally,

another study showed that coating orthopaedic implants with TiO_2 nanoparticles reduced bacterial colonization, with nearly all tested bacteria being eliminated after 50 minutes of UV exposure. The decay kinetics of photokilling observed in their study indicated a two-step process, differing from earlier reports of pseudo-first-order reactions [49].

In energy devices, the progress of nanoscience and nanotechnology has uncovered new chemical and physical characteristics of TiO_2 nanoparticles, paving the way for the development of nano-sized solar cells utilizing TiO_2 [50]. Recent studies have concentrated on synthesizing TiO_2 nanoparticles in various configurations to optimize their surface areas, which enhances the interfacial reactions between the nanoparticles and the surrounding media in photovoltaic systems [51]. Modifications to the surface have been shown to affect energy offsets, charge transport, separation, and recombination processes involving TiO_2 nanoparticles [52]. Among the various forms of TiO_2 nanoparticles, nano-whiskers have been recognized as particularly advantageous for solar cell and windscreen production due to their exceptional charge transport properties [53].

A significant drawback of TiO_2 nanoparticles in semiconductor-based sensing devices is their sensitivity to humidity, which can render sensor responses unreliable in environments with fluctuating humidity levels [54]. This sensitivity is primarily due to the presence of hydroxyl groups on the surfaces of the nanoparticles [55]. In lithium-ion batteries, TiO_2 has emerged as a promising alternative to traditional carbon-based anodes as it offers several advantages, including lower cost, enhanced safety, and reduced toxicity and demonstrates excellent structural stability and a high discharge voltage plateau [56–58]. Additionally, nanostructured TiO_2 serves as a low-voltage insertion host for lithium,

enabling fast insertion/extraction capabilities that make it suitable for high-power applications [59, 60].

In energy production, the production of chemical fuels through the conversion of solar energy is regarded as a crucial strategy for tackling the current global energy crisis [61]. Since the landmark discovery of water splitting on a TiO_2 electrode in 1972 , photocatalysis has attracted considerable attention as a viable method for generating clean, eco-friendly, and cost-effective hydrogen (H_2) using solar energy [62–64]. TiO_2 has emerged as a leading oxide semiconductor photocatalyst for water splitting due to its resistance to chemical and photo-corrosion over time [65–67]. However, pure TiO_2 exhibits relatively low photocatalytic efficiency, making the performance of H_2 production highly dependent on the type and amount of cocatalysts used [68]. This is largely because TiO_2 primarily operates under UV light to bridge the anatase phase band gap (3.2 eV) [69]. Consequently, effective band gap engineering is essential to enhance TiO_2's performance as a semiconductor photocatalyst for improved H_2 production via water splitting and initial efforts involved using cations such as Ag^{2+}, Al^{3+}, Mn^{2+}, Cr^{3+}, Fe^{3+}, and V^{5+} as dopants to introduce new states within the TiO_2 band gap [70]. However, Asahi et al. pointed out various challenges associated with this method, including increased recombination centers, the necessity for low-cost ion implantation, and thermal instability [43]. They suggested nitrogen doping as a more effective strategy for band gap engineering compared to cationic or anionic doping. Nonetheless, subsequent research questioned nitrogen doping's efficacy as the optimal approach noting that the photocatalytic activity of nitrogen-doped TiO_2 for H_2 production was relatively low [71, 72]. To further boost H_2 production from water splitting using TiO_2 nanoparticles,

researchers incorporated platinum (Pt) as a cocatalyst and noted an enhancement in H_2 evolution when sacrificial reagents were present. However, the scarcity and high cost of Pt present significant obstacles to scaling this technique. Park et al. successfully created carbon-doped TiO_2 nanotubes that demonstrated effective H_2 evolution [73].

In another study, Chen et al. explored an alternative method to enhance solar absorption for water splitting by employing black TiO_2 nanocrystals with disordered surface layers achieved through hydrogenation. The TiO_2 nanocrystals were synthesized using a titanium tetraisopropoxide (TTIP) precursor combined with ethanol, deionized water, the organic template Pluronic F127, and hydrochloric acid (HCl). The resulting nanocrystals were calcined at 500°C for six hours to eliminate Pluronic F127 and improve the crystallization of TiO_2. To induce disorder in the nanophase of TiO_2, a porous network of nanocrystals measuring less than 10 nm was hydrogenated. This process shifted the absorption range from UV into the near-infrared (NIR) region and resulted in a noticeable color change. The researchers found that these disorder-engineered nanocrystals exhibited substantial photocatalytic activities, including the photo-oxidation of organic compounds in water and H_2 production using a sacrificial donor under solar illumination [74].

In environmental protection, the use of TiO_2 nanoparticles in wastewater treatment has been recognized as an effective method for breaking down organic pollutants through photocatalysis [75]. Nasikhudin et al. evaluated the effectiveness of TiO_2 nanoparticles for the photodegradation of methylene blue under different pH conditions. The findings showed that the TiO_2 nanoparticles of the anatase phase achieved a remarkable 97% degradation of methylene blue within three hours when exposed to UV light while in the absence of UV light only 15% of the dye had degraded and this was attributed to the

adsorption of the dye by TiO_2 rather than the photocatalytic action [76]. Behnajady et al. investigated the effects of varying precursors and synthesis conditions on the photocatalytic activity of TiO_2 nanoparticles for the removal of organic pollutants [77]. They specifically varied factors such as solvent percentage, reflux time, temperature, drying method, calcination temperature, and water content. The photodegradation of methyl orange (MO), a model textile industry contaminant, was monitored under UV light. Their study demonstrated that the photo-induced degradation of MO by TiO_2 nanoparticles was influenced by the type of solvent, precursor, and other synthesis conditions. In comparison to commercial TiO_2 P25, the TiO_2 nanoparticles synthesized using TTIP as the precursor, methanol as the reflux solvent for three hours at 80°C, followed by thermal drying and calcination at 450°C, showed similar photocatalytic activity [77]. Furthermore, nano-TiO_2 can be anchored onto carbon-based materials such as carbon nanotubes (CNTs), graphene, and carbon nanofibers to create nanohybrids that demonstrate enhanced photocatalytic performance for wastewater treatment [78, 79]. Carbon-based materials are particularly well-suited for supporting TiO_2 due to their chemical resistance, mechanical strength, thermal, electrical, and optical properties [80, 81].

In industrial applications, TiO_2 has attracted attention due to the high refractive indices of the rutile (2.70) and anatase (2.55) crystalline phases of TiO_2 which have the ability to scatter light prominently and for this reason it has been used as white pigment in plastic, paper, coatings and ink [82]. In coating applications, TiO_2 is used as a film or paint on different surfaces such as buildings, wood and metals to cover the surface depending on their specific uses [83]. In plastic applications, TiO_2 is added in order to make the plastic

less transparent and in the paper industry, TiO_2 is used as the white pigment in paper as it makes paper brighter and opaquer and and papers with TiO_2 are usually white, shiny, thin, and smooth. Since paper doesn't need to resist light as much as paint, both types of TiO_2 anatase and rutile are commonly used [82, 84].

2.4 TiO_2 as an anti-soiling coating

In addition to its numerous applications, TiO_2 has also been used as an anti-soiling/self-cleaning coating due to its effectiveness in enhancing surface cleanliness [26]. The self-cleaning properties of TiO_2 stem from two mechanisms namely photocatalysis and hydrophilicity/hydrophobicity [85, 86]. Photocatalysis is a process that requires both light and a catalyst, with TiO_2 playing a crucial role in initiating chemical reactions through this mechanism [87]. The photocatalytic process begins when UV light with photon energy equal to or greater than the band gap of TiO_2 is absorbed, causing an electron to jump from the valence band to the conduction band, which leaves a positively charged hole in the valence band [88]. These charge carriers then engage in redox reactions with molecules adsorbed on the TiO_2 surface where the hole acts as a strong oxidizing agent, while the electron acts as a reducing agent. The hole reacts with water (H_2O) or hydroxyl ions (OH^-) to produce hydroxyl radicals ($OH\bullet$), which are powerful and non-selective oxidants capable of degrading pollutants into H_2O and CO_2 [89]. Simultaneously, the electron in the conduction band reduces adsorbed oxygen (O_2) to superoxide radicals ($O_2\bullet$), which can further react to generate additional $OH\bullet$ radicals which interact with organic pollutants and harmful microorganisms leading to their breakdown [90]. If the electron-hole pairs recombine before they can react, energy is released as heat, which reduces the efficiency

of TiO_2 photocatalysis [91]. This recombination process competes with the redox reactions of electron donors and acceptors and can occur in either the semiconductor bulk or at its surface, releasing heat and diminishing photocatalytic performance [92]. **Figure 2.3** shows a diagram depicting the self-cleaning process, highlighting how organic contaminants are degraded when exposed to sunlight [85].

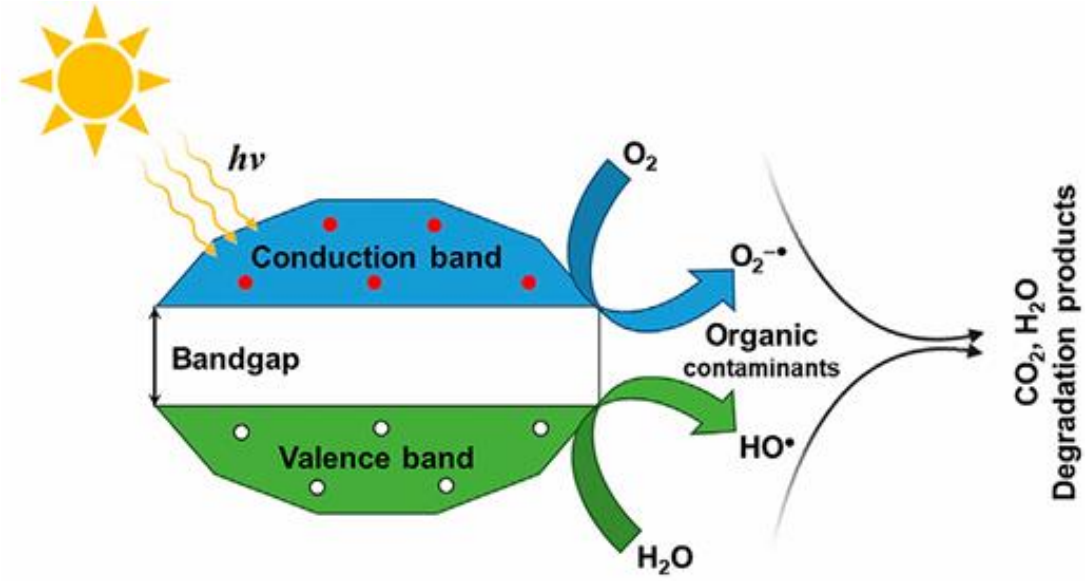

Figure 2.4 Schematic representation of the self-cleaning mechanism by degradation of organic contaminants.

A study by Komaraiah et al. demonstrated the photocatalytic degradation of methyl blue (MB) aqueous solution in the presence of visible light illumination for 4 hours with TiO_2 thin films as the catalyst. The TiO_2 was deposited onto glass substrate via the sol-gel spinning method and these thin films demonstrated 92% MB degradation efficiency [93]. Another study by Hassen et al investigated the photodegradation of MO by TiO_2 . The results showed the decolorization of MO in 300 minutes in the presence of UV light which indicates that TiO_2 is highly effective in breaking down the MO in the presence of UV light [94].

TiO_2 is primarily hydrophilic, and its hydrophilicity arise mainly from two mechanism [95]. Firstly, under illumination, hydroxylation occurs on the surface of TiO_2 creating hydroxyl anions as well as oxygen vacancies. During photocatalysis, the hydroxyl ions bond onto the oxygen vacancies creating the hydrophilic nature of TiO_2 [96]. Additionally, the holes generated during photocatalytic degradation migrate to the surface of TiO_2 where they get trapped into the oxygen vacancies as well and form hydroxyl anions in the presence of water, further inducing the hydrophilic nature of TiO_2 [52, 97].

The second mechanism pertains to the breakdown of contaminants on the surface of TiO_2 in addition to photodegradation where UV illumination can trigger the desorption of loosely bound water molecules from the TiO_2 surface in which the Ti-O-Ti bonds are easily broken by water molecules to form two new Ti-OH bonds which further transforms the surface into a hydrophilic state [97, 98]. A study by Lukong et al. investigated the deposition and characterization of TiO_2 thin films for self-cleaning applications in photovoltaics. The thin films fabricated via spin coating on glass substrate demonstrated hydrophilic properties with a WCA of 37.30^{o} and the self-cleaning test done by the photocatalytic degradation of MB showed that TiO_2 thin films were able to degrade 90% of the dye after 120 minutes of exposure to UV light proving that TiO_2 thin films are effective in self-cleaning applications [99]. In a separate study by Lopes et al. assessment of the anti-soiling performance of TiO_2 coatings on concentrated solar power (CSP) mirrors was done which revealed that the coating did not have any effect on the reflectivity of the CSP mirror and exhibited great endurance [100].

2.5 Effect of doping on TiO_2

The application of TiO_2 is limited to its UV light absorption due to its wide band gap [101]. For this reason, researchers have attempted to shift the sensitivity of TiO_2 by doping it with various elements [102]. Doping refers to the introduction of impurities into the TiO_2 lattice in order to modify and improve its properties [103]. These modifications include improving the optical properties of TiO_2 which increases its sensitivity in the visible region and further expands its applications [104]. Surface modification by doping also reduces the recombination of electron and holes generated in the presence of light by increasing the charge separation in return increasing the photocatalytic efficiency of TiO_2 [105].

TiO_2 has been previously doped with various metals including Aluminium (Al), Zinc (Zn) and Copper (Cu) to improve its properties. Al for instance is known to improve the electrical properties of TiO_2 by increasing the density of states (DOS) near the fermi energy level that results in higher density of charge carriers [106]. Furthermore, Al increases light transmittance of TiO_2 by reducing the surface trap state of TiO_2 which traps electron and limit their movement [107]. Zn has been introduced as an effective dopant into TiO_2 due to its ability to improve the electrical as well as the optical transparency of TiO_2 and overall increase the photocatalytic efficiency of TiO_2 by preventing the recombination of photogenerated electron and holes [108, 109]. The incorporation of Cu into TiO_2 can increase the interaction of photogenerated electrons and holes with compounds on the surface of TiO_2 due to Cu being able to reduce electron-hole recombination [110]. The decrease in the recombination rate of electron-hole pairs can be attributed the reduction in the band gap of TiO_2 by Cu [111, 112]. Additionally, Cu is also

able to modify the energy adsorption of TiO_2 which improves its optical properties[111]. In a study reported by Pava et al, Cu-doped TiO_2 thin films fabricated via the sol-gel method were able to increase the degradation efficiency of undoped TiO_2 thin films from 2.6% to 25.1% by the degradation of MO after 6 hrs [113]. In another study by Bensouici et al, Cu-doped TiO_2 thin films deposited via the sol-gel method demonstrated a decrease in optical band gap energy with increasing Cu concentration indicating the ability for Cu to enhance the visible light absorption and photocatalytic efficiency of TiO_2 [114]. In a separate study Zn-doped TiO_2 thin films prepared by sol-gel showed a decrease in band gap energy of TiO_2 from 3.10 eV to 3.83 eV and the study on also revealed that films with 2 wt% and 4 wt% Zn, annealed at 300 °C and 400 °C, exhibit hydrophilic properties, with water contact angles ranging from 22° to 54° suggesting that the incorporation of Zn and controlled annealing significantly enhance the hydrophilicity and photocatalytic efficiency of Zn-doped TiO_2 thin films, making them promising candidates for self-cleaning applications [115]. Although TiO_2 has been doped with other metals such as nitrogen (N), Nickel (Ni) and Tin (Sn) etc. Al, Zn and Cu pose as sustainable dopant materials due to their non-toxicity, availability and cost effectiveness [108, 112].

2.6 Established methods for the fabrication of thin films

One of the critical aspects of utilizing thin films is their fabrication with precise control over their properties [116]. The method of fabrication has great impact on the outcome of the uniformity, thickness and composition of the thin films [117]. The fabrication methods can be divided into two, namely physical and chemical deposition techniques.

Physical deposition includes magnetron sputtering and pulsed laser deposition (PLD) techniques which involve vaporizing as solid material in a vacuum environment which is further deposited onto a substrate to create the thin film [117, 118]. Thin films created through these techniques are often highly durable, of high quality and resistant to corrosion. However, their drawbacks include costly and complex high ultra-high vacuum systems that are needed for the deposition process, and they also have slow deposition rates as well as low deposition rates [118–120].

Chemical deposition techniques include but are not limited to, chemical vapor deposition (CVD), atomic layer deposition (ALD), sol-gel, spin coating and spray coating [120]. CVD involves chemical reactions whereby compounds of a gaseous phase diluted with an inert carrier gas decompose on the surface of a heated substrate to form a solid film [117, 118, 120]. CVD produces high-quality films with good uniformity and high deposition rates. However, it requires very high temperatures as well as expensive and complicated equipment for production and their by-products are hazardous [119–121]. In ALD two or more gaseous precursors react on the surface of the substrate in a sequential manner to produce the thin film [120]. Thin films fabricated through these methods are often of good quality, have excellent adhesion and do not require high temperatures for production. However, they have low deposition rates and suitable chemical precursors are rare [119, 120].

Sol-gel is one of the most common and broadly used techniques in the fabrication of thin films [122]. It involves hydrolysis and partial condensation of metal precursors to form a liquid colloid suspension called sol which further undergoes condensation to form a gel hence the name sol-gel [120]. Although sol-gel uses simple and cost-effective equipment,

uses low temperatures and has high adhesion strength, it makes use of harmful; organic compounds, involves high cost of raw materials and chemical precursors are not stable against hydrolysis and side reactions [119, 120]. In the spin-coating technique, the precursor solution is deposited into the center of the substrate and the substrate is spined at high speed to form uniform thin films [118]. These methods produce thin films with high uniformity, use simple and cost-effective instrumentation however it cannot produce thin films on a large scale and wastes the precursor solution during spinning [120]. The spray coating method involves the deposition of an aqueous precursor solution onto a preheated substrate through a spray nozzle using compressed air as a carrier gas to form thin films [118, 119].This method has grown as an emerging fabrication method over other methods due to its low production cost, high growth rate, high quality adherent films with uniform thickness, flexibility of substrate choice and its ability to produce thin films on a large scale [118, 120, 123].

2.7 TiO_2-based thin films fabricated by the aqueous spray method.

Due to its instrumentation and low costs, the aqueous-spray method has been used to fabricate TiO_2 thin films. In a study conducted by Kadhingula, the fabrication of TiO_2 and TiO_2/Ag composite thin films fabricated via the aqueous spray method was investigated. The study focused on preparing precursor solutions involving Ti^{4+} and Ag^{2+} complexes to prepare thin films, also emphasizing the spray method as a cost-effective approach to produce TiO_2 thin films for its applications in nanotechnology. The resultant thin films yielded more than 80% transmittance validating the method's potential for functional material production [124]. In a different study by Mutenda, the fabrication of TiO_2 thin

films using the spray coating methods was investigated where precursor solution containing Al^{3+} and Ti^{4+} complexes were spray-coated onto pre-heated glass substrates yielding Al-doped TiO_2 with improved transmittance [125]. Another investigation led by Giolando focused on developing a transparent self-cleaning coating for solar energy applications, consisting of titanium dioxide nanocrystals embedded in fluorine-doped tin dioxide fabricated via the aqueous spray method. The resultant coated glass demonstrated high transmittance in the visible region and exhibited increased abrasion resistance and stability under certain temperatures and these results suggested that the self-cleaning coatings can enhance the performance of solar energy devices [126].

CHAPTER 3

Materials and Methods

3.1 Chemicals

The chemicals used in this study were oxalic acid ($H_2C_2O_4$), ammonium oxalate $(NH_4)_2C_2O_4$, 97% titanium (v) butoxide ($Ti(OBu)_4$), 1-propanol, 100% hydrogen peroxide (H_2O_2), aluminum nitrate nonahydrate ($Al(NO_3)_3.9H_2O$), zinc acetate ($Zn(CH_3COO)_2$) , 25% ammonium hydroxide (NH_4OH), copper acetate ($Cu(CH_3COO)_2$ and methyl orange (MO). All chemicals were used without further modification and all solutions were prepared using distilled water and the ethical clearance certificate was obtained from the university of Namibia ethics committee o the 20th of September 2024.

3.2 Preparation of ammonium titanyl oxalate monohydrate $(NH_4)_2[Ti(C_2O_4)_2O]\cdot H_2O$ (Ti^{4+} complex)

Ammonium titanyl oxalate monohydrate $(NH_4)_2[Ti(C_2O_4)_2O]\cdot H_2O$ was not readily available. Therefore, it was prepared from scratch in order to obtain a Ti^{4+} complex that was used to prepare Ti^{4+} precursor solutions. $(NH_4)_2[Ti\ (C_2O_4)_2O]\cdot H_2O$ was prepared according to previous methods done by our research group.

In a beaker, $(NH_4)_2C_2O_4$ (1.8863 g) was dissolved in distilled H_2O (50.0000 g) by heating at 80°C while stirring with a magnetic stirring bar (hot plate setting 698 RPM). After it had completely dissolved, $H_2C_2O_4$ (1.9162 g) was added to it while stirring and heating continued until $H_2C_2O_4$ had also completely dissolved. $Ti(OBu)_4$ (5.1546 g) was then gradually added to the mixture and the solution was left to stir while heating at 80°C for 1 hour. After 1 hour the solution was expected to be clear. However, it was turbid (cloudy)

therefore a small amount of oxalic acid was added and the solution turned clear [127]. After the solution had turned clear it was removed from the hot plate and immediately 1-propanol twice as much as the solution was added while stirring with a stirring rod until a white powder formed which was suspected to be the $(NH_4)_2[Ti\ (C_2O_4)_2O]\cdot H_2O$ (Ti^{4+} complex) product. It was then filtered with a Buchner funnel and washed severely before it was left to dry in a desiccator for about 1 hour.

3.3 Preparation of undoped Ti^{4+} precursor solution

The Ti^{4+} complex previously obtained in **3.2** was used to prepare an undoped Ti^{4+} precursor solution. This was achieved by mixing the Ti^{4+} complex (0.5978 g) with 100% hydrogen peroxide (H_2O_2) (0.0691 g) and distilled water (40.0000 g). The concentration of the solution was kept at 0.05 mmol/g. This solution was the stirred for 1 hour at room temperature.

3.4 Preparation of Al^{3+}, Zn^{2+} and Cu^{2+} precursor solutions

The precursor solution containing Al^{3+} complexes was prepared by dissolving 0.1110 g of $Al(NO_3)_3\cdot 9H_2O$ in 10.0000 g of distilled water. Similarly, the Zn^{2+} precursor solution was formulated by combining 0.1166 g of $Zn(CH_3COO)_2$ with 0.5066 g of NH_4OH and 10.0000 g of distilled water. For the Cu^{2+} precursor solution, 0.0935 g of $Cu(CH_3COO)_2$ was mixed with 0.2106 g of NH_4OH and 10.0000 g of distilled water.

All solutions were stirred for one hour at room temperature, maintaining a concentration of 0.05 mmol/g throughout.

3.5 Preparation of Al, Zn and Cu-doped Ti^{4+} precursor solutions

The precursor solution containing only Ti^{4+} complexes was regarded as the 0% doped Ti^{4+} solution. Ti^{4+} doped precursor solutions were prepared by taking 9.8 g of the Ti^{4+} precursor

solution and combining it with 0.2 g of the Al^{3+} precursor solution resulting in the total mass of 10 g. This was done in order to achieve 2% Al-doped Ti^{4+} precursor solution. This process was repeated for 4%, 6%, 8%, and 10% Al-doped solutions by adjusting the amounts of Ti^{4+} and Al^{3+} precursor solutions accordingly where for instance, to make a 4% Al-doped solution, 9.6 g of Ti^{4+} and 0.4 g of Al^{3+} was used to make a total mass of 10g. The same method was also applied to prepare Zn-doped Ti^{4+} precursor solutions. However, with Cu, the initial plan was to prepare Cu-doped Ti^{4+} solutions with five different doping concentrations of 2%, 4%,6%, 8%, and 10% but during the preparation process, it was observed that the 8% and 10% Cu-doped solutions were not clear and exhibited cloudiness, making them unsuitable for spray as the cloudiness could compromise the quality and uniformity of the resulting thin films. As a result, the study proceeded with only the three clear solutions (2%, 4%, and 6%) of Cu-doped Ti^{4+}.

3.6 Fabrication of TiO_2-based thin films

Before fabrication of the thin films, quartz glass substrates were prepared by ultrasonicating them in soapy water for 30 minutes. They were subsequently scrubbed with a sponge, rinsed with distilled water, and ultrasonicated again in distilled water for another 30 minutes. After rinsing with distilled water, the substrate was placed in isopropyl alcohol (IPA) and ultrasonicated for 30 minutes. It was then rinsed with IPA, ultrasonicated in IPA for an additional 30 minutes, and finally stored in IPA.

The undoped, Al, Zn and Cu-doped precursor solutions were used as the coating solutions and spray-coated onto the pre-heated quartz glass substrates of 20 × 20 mm^2 , using identical experimental set up from previous work done by our research group as shown in **Figure 3.1** [125].

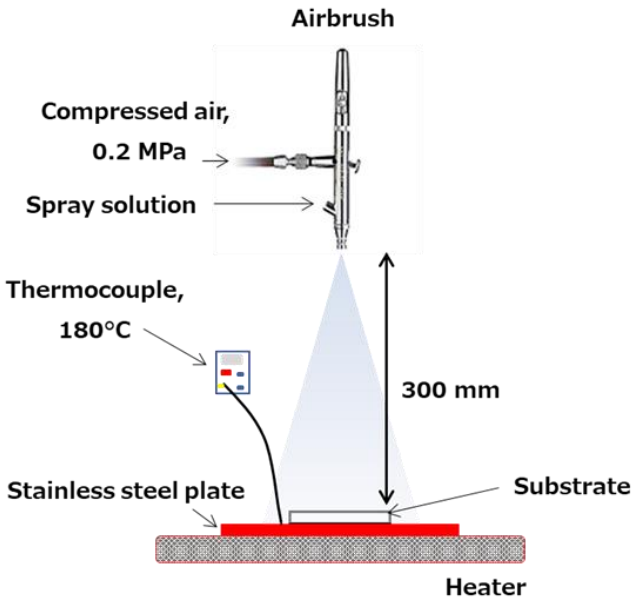

Figure 3.1 Illustration of spray-coating set-up

The quartz glasses were placed on a stainless-steel plate of a hotplate and the temperature of the hot plate was controlled and monitored at 180℃ using a thermocouple thermometer. 6 g of each coating solution was spray-coated onto the pre-heated quartz glass using an airbrush (HP-SAR; ANEST IWATA Co., Kanagawa, Japan) with compressed air of 0.2 MPa as a carrier gas, spraying for 5s at 20s intervals and at a spraying rate of 0.49 g/min. The distance between the tip of the airbrush and substrate was kept at 300 mm.

3.7 Heat-treatment

For annealing, the as-sprayed thin films were placed into crucibles heat-treated at 500℃ for 30 minutes in a separation muffle furnace and thereafter left to cool at room temperature.

3.8 Characterisation

Fourier Transform Infrared Spectroscopy (FT-IR) which was carried out to identify and confirm the bonds in the synthesized $(NH_4)_2[Ti\ (C_2O_4)_2O]\cdot H_2O$. The fabricated thin films were characterized using various techniques. The crystal structure of all the thin films were determined utilizing X-ray diffraction (XRD) using a SmartLab X-ray diffractometer (Rigaku, Tokyo, Japan). Parallel beam optics at an incident angle of 0.3° was used in the 2θ range of 10–80°. The optical transmission spectra of the thin films were measured using the UV-Vis (PerkinElmer UV/VIS spectrometer) analysis in the spectral range of 200-1100nm to assess their interaction with light in the visible region.

3.9 Photocatalytic Activity of the TiO_2 thin films

The photocatalytic activities of the prepared thin films were investigated by degradation of MO dye. The thin films were immersed in 4 mL methyl orange solution contained in a cell. The initial concentration of the methyl orange was kept at 8 mg/L. A xenon lamp with visible light was used as the light source and the distance between the light source and the cell was 25.5 cm. Before the lamp was turned on the dispersion was placed in the dark for 30 minutes to reach ad/desorption equilibrium. After the ad/desorption equilibrium, the lamp was then turned on for 4 hours of irradiation. UV-vis spectrophotometer was used to assess the absorbance of the dye after irradiation. The beer lambert's law in equation 1 was used to obtain the concentration of the dye after irradiation.

$$A=\varepsilon\cdot C\cdot l$$

Where A is the absorbance, ε is the molar absorptivity, C is the concentration and l is the path.

After the concentration was determined, the degradation efficiency of the thin films was determined using the following equation

$$\text{Degradation efficiency} = (C_0\text{-}C/C_0)\times 100$$

Where C_0 was the initial concentration of MO before irradiation, and C was the concentration of the MO after irradiation

CHAPTER 4

Results and Discussion

4.1 Prepared precursor solutions and resultant thin films

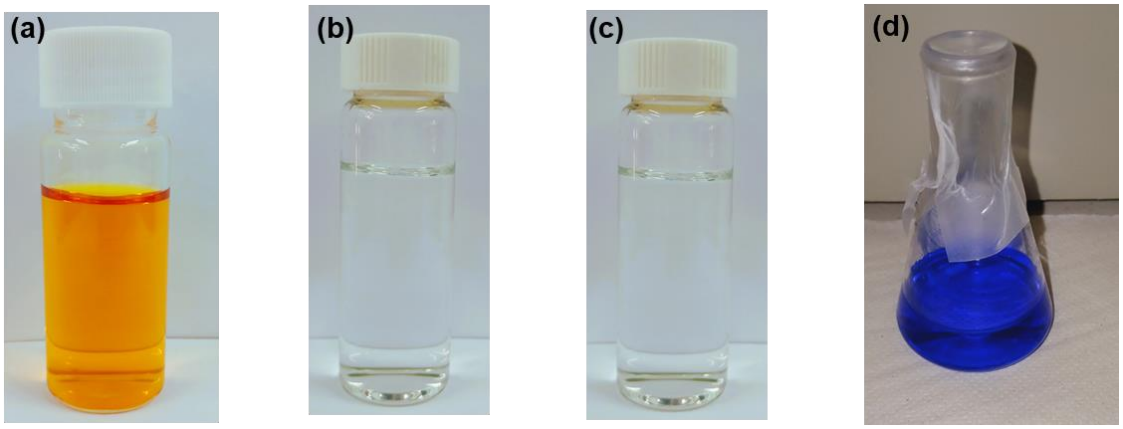

Figure 4.1 Precursor solutions contain (a) Ti^{4+} (b) Al^{3+} (c) Zn^{2+} and (d) Cu^{2+} ions

The precursor solution containing Ti^{4+} had an orange color (**Figure 4.1**) which is an indication of the presence of Ti^{4+} ions [124]. The Al^{3+} and the Zn^{2+} precursor solutions were clear solution while the Cu^{2+} solution was blue. **Figure 4.2** shows the Al, Zn and Cu-doped precursor solutions used to fabricate the thin films and Figure 4.3 shows the fabricated thin films.

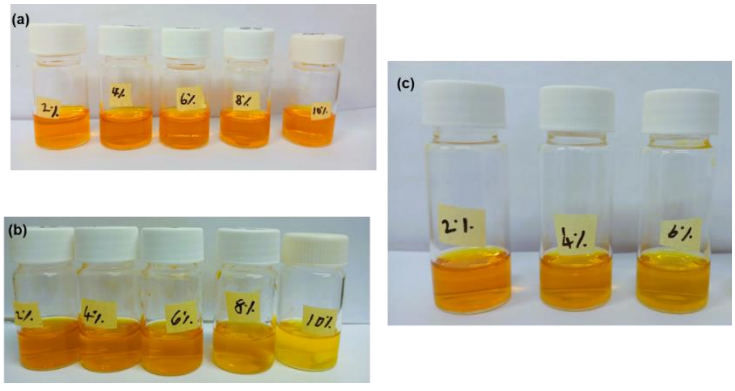

Figure 4.2 (a) Al-doped Ti^{4+} precursor solutions, **(b)** Zn-doped Ti^{4+} precursor solutions and **(c)** Cu-doped Ti^{4+} precursor solutions

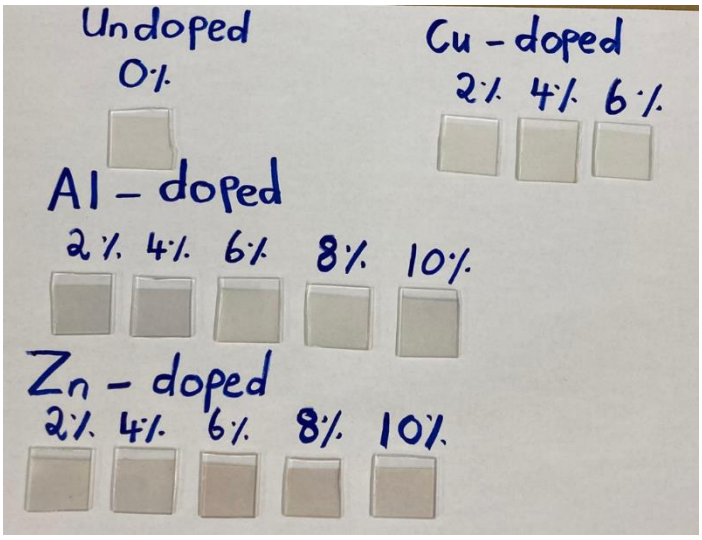

Figure 4.3 Fabricated thin thins

4.2 Characterisation of the synthesized $(NH_4)_2[Ti(C_2O_4)_2O]\cdot H_2O$

The FT-IR spectrums of oxalic acid and ammonium oxalate were used as baselines for identifying the functional groups in the Ti^{4+} complex as shown in **Figure 4.4**. Oxalic acid showed characteristic O-H stretching band around 3495 cm^{-1} as well as C=O stretching band around 1686 cm^{-1}. In the ammonium oxalate, N-H stretching band were observed around 3196 cm^{-1} as well as C=O and C-O stretching bands between 1130 cm^{-1} and 1630 cm^{-1}. In the Ti^{4+} similar O-H peaks were observed, but with slight shifts, indicating coordination with Ti^{4+} ions. Additionally, the appearance of Ti–O bond peaks around 650 cm^{-1} confirmed the complex formation, with the overlapping and shifted peaks from oxalic acid and ammonium oxalate.

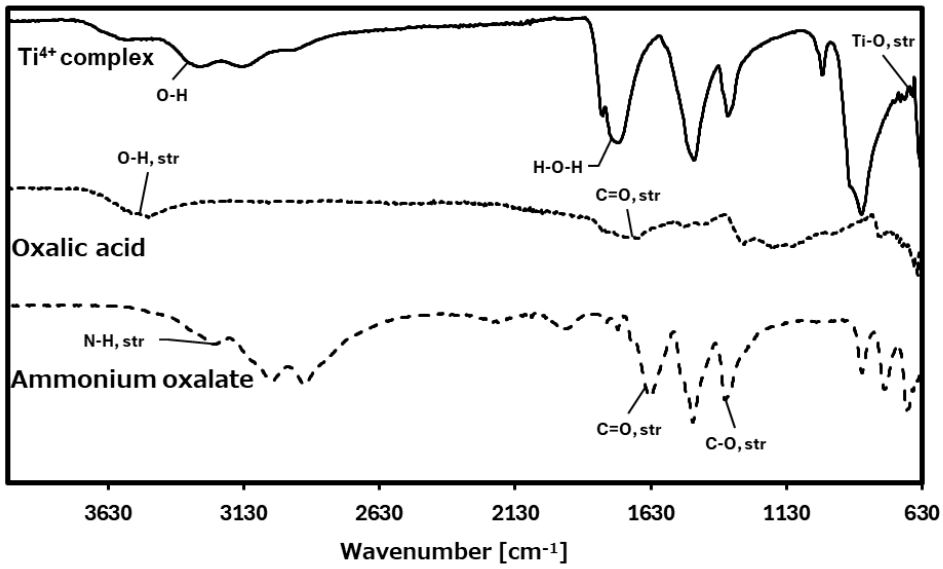

Figure 4.4 FTIR spectra of ammonium oxalate, oxalic acid and ammonium titanyl oxalate monohydrate

4.2 Crystal Structures

The structural properties of the prepared thin films were obtained using XRD. **Figure 4.5** demonstrates the diffractogram of the undoped and Al-doped TiO_2 with the observed diffraction peaks at 2θ of 25.30° assignable to characteristic peaks of anatase TiO_2 (101). No additional peaks attributable to Al species were observed which could suggest the successful incorporation of Al into the TiO_2 lattice without disturbing its structure [128]. Additionally, it has been observed that the intensity and sharpness of the peaks increases with increasing doping percentage from 2% to 10% Al-doping. This can be attributed to the high physical stressing on the lattice with increasing Al incorporation into the TiO_2 structure and could imply the enhancement of the crystal growth [128, 129].

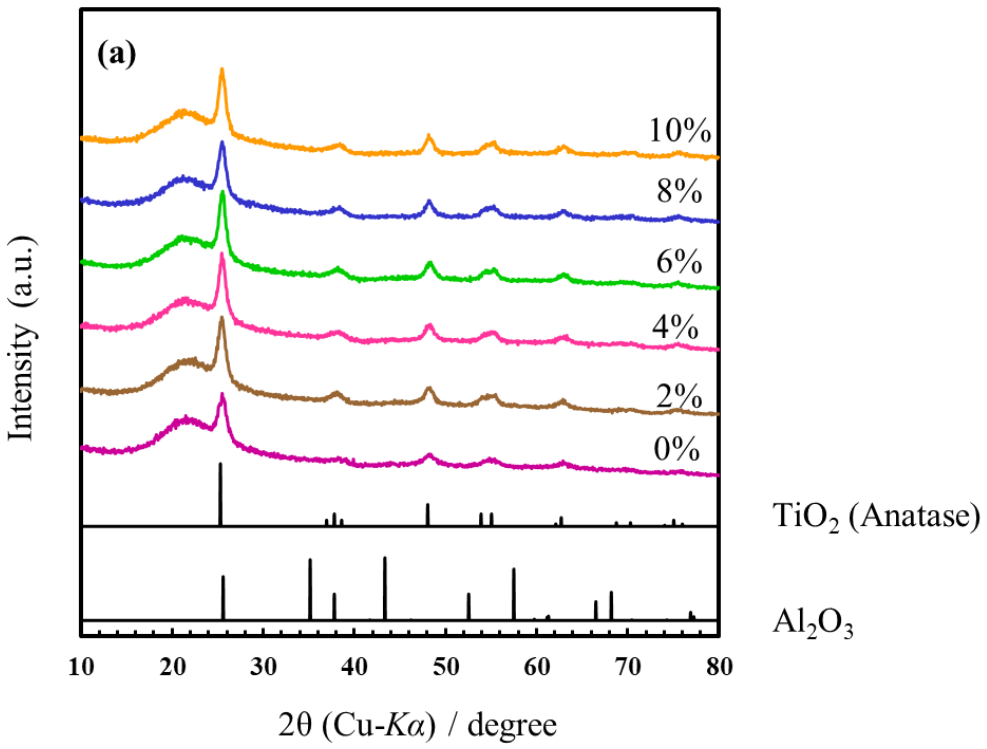

Figure 4.5 XRD diffractogram of undoped and Al-doped TiO_2 thin films

Similarly, the structural properties of the Zn- and Cu-doped TiO_2 thin films were also investigated using XRD shown in **Figures 4.6** and **Figure 4.7** respectively. As with Al doping, the Zn and Cu-doped samples exhibited diffraction peaks corresponding to the anatase phase of TiO_2, with no additional peaks detected which may be attributable to Zn or Cu species, indicating their successful incorporation into the TiO_2 lattice without significant structural disruption. However, for the Cu-doped TiO_2 films, the intensity of the anatase peaks was notably higher compared to those of the Al- and Zn-doped samples. This suggests that Cu doping exerted greater stress on the lattice, promoting enhanced crystal growth and leading to sharper and more intense anatase peaks than those observed with Al or Zn doping.

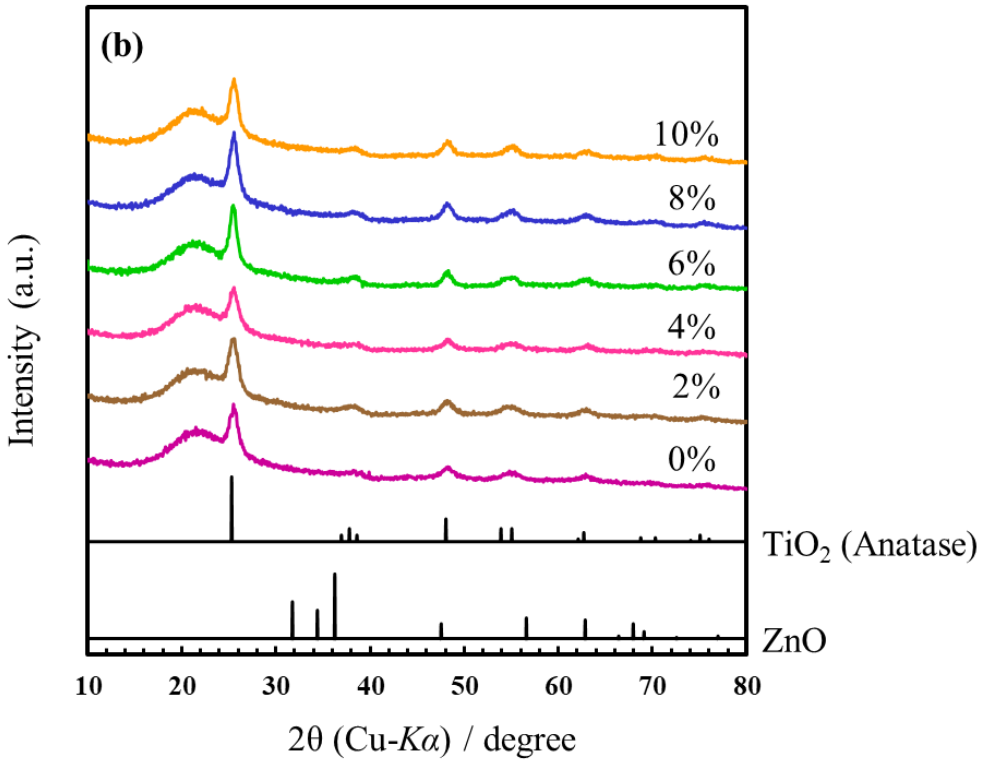

Figure 4.6 XRD diffractogram for undoped and Zn-doped TiO2 thin films

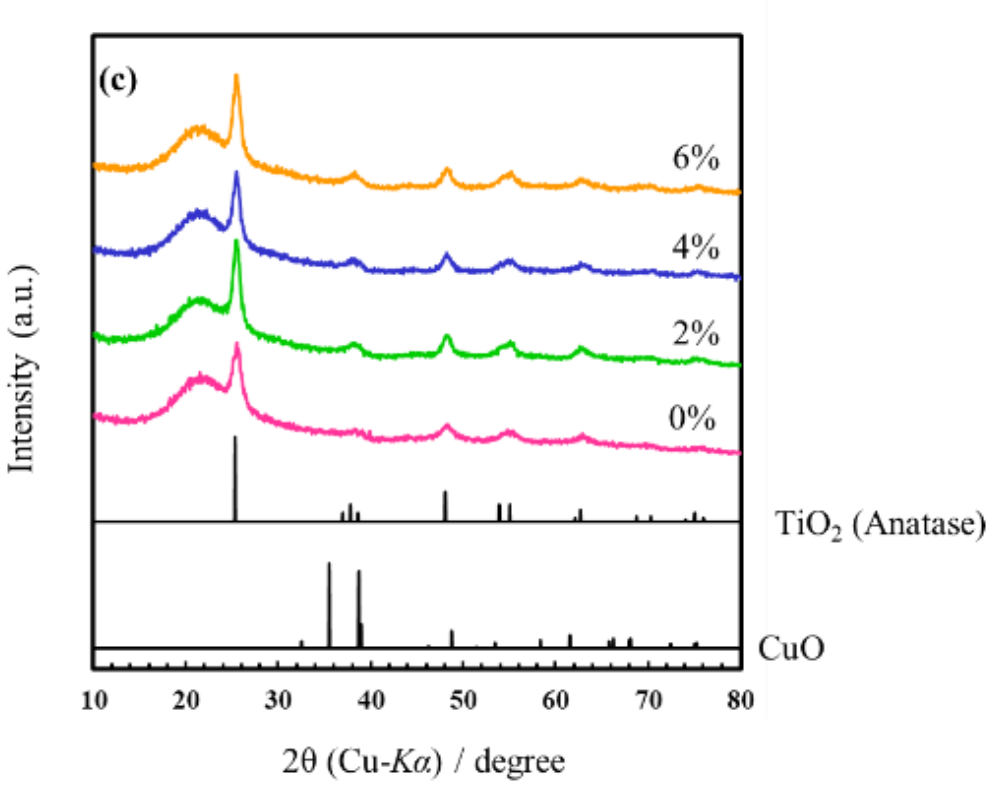

Figure 4.7 XRD diffractogram for undoped and Zn-doped TiO2 thin films

4.3. Optical properties

The transmittance spectra of the undoped and Al, Zn and Cu-doped thin films were studied to evaluate the effects of doping on the optical properties of TiO_2 and the transmittance was notably higher in the visible region and near infra-red region (NIR) while lower at wavelengths below 400 nm. **Figure 4.8** shows the transmittance spectra of undoped and Al-doped TiO_2 thin films. The transmittance is higher in the visible region and lower at wavelength below 400 nm. The transmittance of the undoped TiO_2 thin film is about 78%.

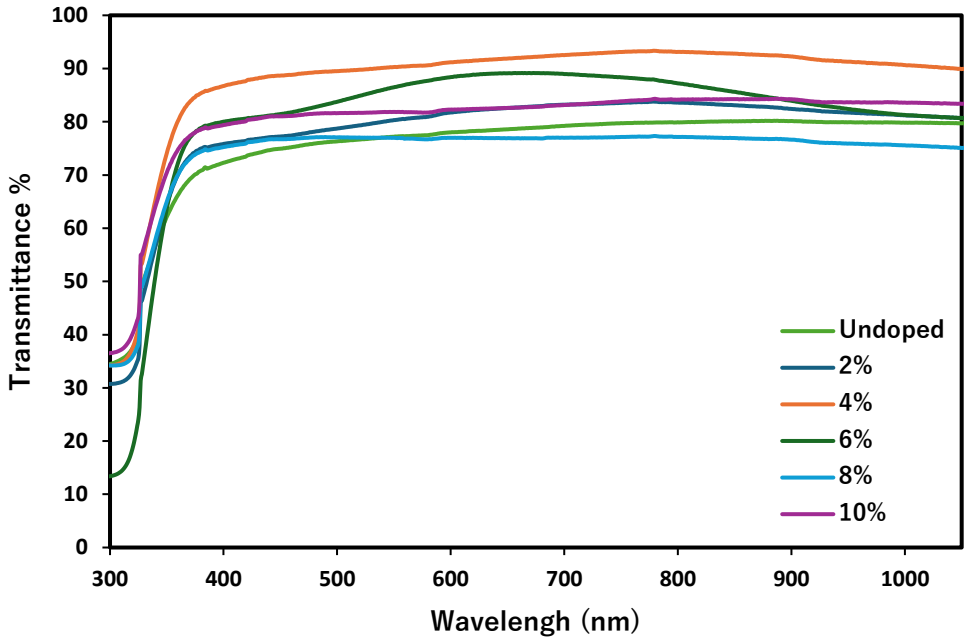

Figure 4.8 UV-vis transmittance spectra of Al-doped TiO_2 thin films at different doping concentrations.

The highest transmittance achieved by the Al-doped thin films was 92% for 4% doped thin films, followed by 6% with 89% while both 2% and 10% both increased the transmittance with 83%. Anjum et al. noted that inconsistency of the increase in transmittance with Al-doping percentage can be attributed to the fact that transmittance is influenced by various factors including surface morphology such as smoothness and roughness of the thin films, deposition technique, thickness as well as material with the lower achieved transmittance such as those achieved by the 2% and the 10% being attributed to highly agglomeration of grains and undecomposed materials [108].

Interestingly, the 8% Al-doped thin films had the lowest transmittance of 77% which is lower than the undoped TiO_2 meaning that Al has decreased the transmittance of TiO_2. This observed trend aligns with findings documented in the existing literature and is

attributed to increased photon scattering caused by crystal defects, as well as free carrier absorption from excess doping materials [130]. Despite the fluctuations, the overall the effect of Al-doping on the optical transmittance of TiO_2 improves with specific doping levels and the variation in transmittance with different doping concentrations suggests that Al is a promising dopant for improving the transmittance of TiO_2 with variable doping concentrations.

The optical transmittance of undoped and Zn-doped TiO_2 thin films, as illustrated in **Figure 4.8**, demonstrates an improvement in transmittance with the introduction of Zn doping. Notably, the 2% Zn-doped thin film exhibits a significant increase in transmittance, reaching 89%, compared to the 78% transmittance of the undoped films. This increase in light transmission highlights the beneficial impact of low-level Zn doping. Although a slight reduction in transmittance is observed at 4% Zn doping, with 88%, and continues to decline marginally at higher concentrations of 6%, 8%, and 10% doping levels resulting in 86%, 87%, and 87%, respectively however these values remain higher than the undoped counterpart, underscoring the overall enhancement.

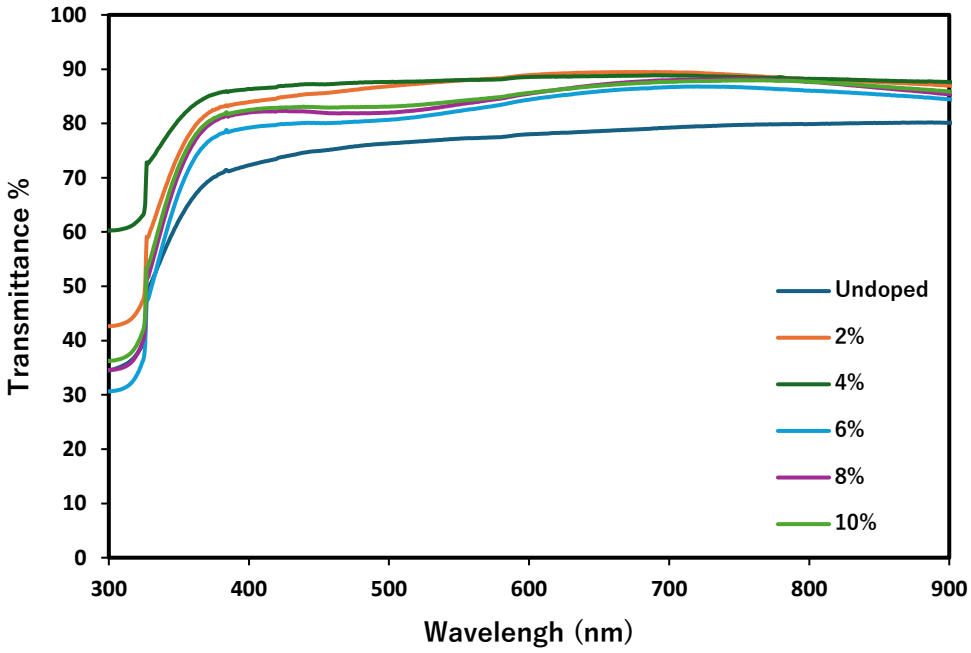

Figure 4.9 UV-vis transmittance spectra of Zn-doped TiO_2 thin films at different doping concentrations

According to Anjum et al. the decrease in transmittance with increasing doping concentrations of Zn can be attributed to significant grain agglomeration and the presence of undecomposed material [108]. These results suggest that Zn doping can enhance the optical properties of TiO_2, but careful optimization of the doping level is required to achieve maximum transmittance.

The transmittance spectra of Cu-doped TiO_2 thin films, as shown in **Figure 4.10** reveal a trend with doping concentration. The 2% Cu-doped TiO_2 thin films exhibited the highest transmittance, reaching 92%, followed by the 4% and 6% Cu-doped films, which displayed transmittance values of 85% and 83%, respectively.

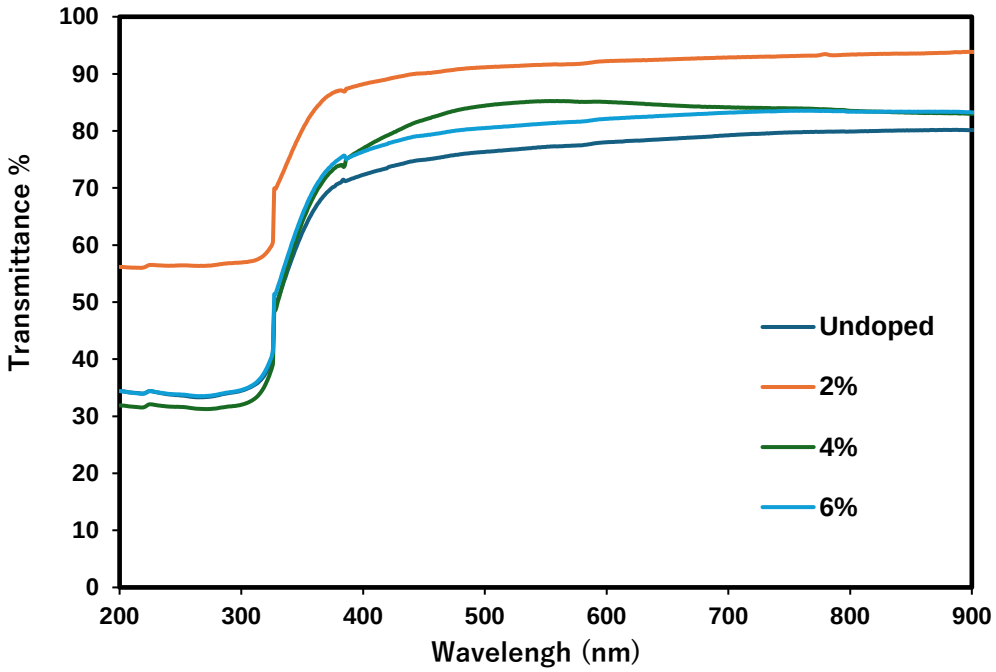

Figure 4.10 UV-vis transmittance spectra of Cu-TiO_2 thin films at different doping concentrations

This decrease in transmittance with increasing Cu concentration suggests that lower levels of Cu doping effectively enhance the optical properties of TiO_2. The significant transmittance at lower doping concentrations points to an optimal balance between Cu incorporation and light transmission, where minimal doping improves the film's transparency, while excessive doping may introduce defects or scattering centers, reducing transmittance.

4.4 Photocatalytic activity

The photocatalytic activities of the undoped and doped TiO_2 thin films was analysed by the degradation of MO under visible light. After irradiation, a noticeable reduction in the initial volume of MO used in the experiment was observed. According to Kriel et al. the reduction in the volume changes can be attributed to evaporation that occurs during the process. To maintain consistency in experimental conditions and ensure accuracy in the results, Kriel has recommended reinstating the amount of solute (water) lost during irradiation to compensate for the evaporated volume.

Figure 4.11 shows the absorbance spectra of the MO before irradiation as well as MO after 4 hours of irradiation in the presence of undoped and Al-doped TiO_2 thin films. The absorbance of the MO before irradiation was found to be 0.4844 and all absorbance values of each MO solution was measured at 468 nm. The results indicate that the absorbance of the MO changes with different doping levels. The absorbance of MO irradiated in the presence of undoped TiO_2 thin films decreased from 0.4844 (before irradiation) to 0.4152, indicating that the undoped TiO_2 effectively facilitated the reduction of MO absorbance in solution [131].

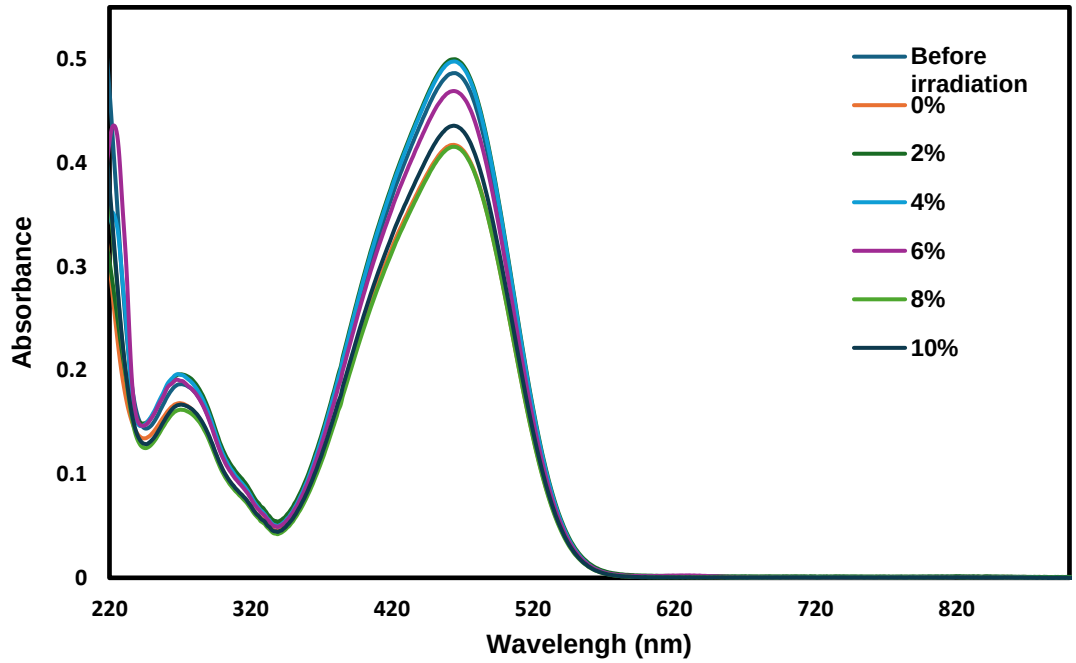

Figure 4.11 MO orange absorbance spectra before and after photocatalysis in the presence of undoped and Al-doped TiO_2

Interestingly, 2% and 4% Al-doped TiO_2 showed an increase in absorbance to 0.4978 and 0.4955 respectively suggesting an apparent increase in the final concentration of the MO after irradiation. This has been previously attributed to the formation of intermediate species during the degradation process. According to Beydaghdari et al, a high initial concentration of the dye can lower photodegradation efficiency by saturating the active sites on the photocatalyst surface, reducing photonic efficiency. As MO undergoes partial degradation, these intermediate species accumulate and can bind to the surface, occupying active sites. Additionally, these intermediates may exhibit absorbance in a similar wavelength range as MO, thereby appearing as an increase in MO concentration [132]. This effect results in a misleadingly high absorbance reading, as the spectrophotometer detects both MO and intermediate species, making it seem as though the concentration of

the dye has increased rather than decreased. Consequently, the apparent increase in absorbance with 2% and 4% Al-doping could indicate that photocatalytic efficiency was limited by site saturation and the accumulation of intermediates, which masked the actual degradation progress of MO. Doping at 6% slightly reduced absorbance to 0.4670, showing minor improvement. 8% Al-doped TiO_2 achieved the lowest absorbance of 0.4136, comparable to undoped TiO_2, indicating an increase in the photocatalytic effect on MO. Finally, 10% Al-doped TiO_2 exhibited an absorbance of 0.4337, which had some degradation, but reduced efficiency compared to the 8% Al-doped. Overall, these findings suggest that undoped or moderately doped TiO_2 (particularly around 8%) may offer better photocatalytic performance, with lower and higher doping levels having limited or adverse effects. The decrease in absorbance by the 6% and the 10% Al-doped TiO_2 thin films can be attributed to electron-hole recombination that occurs before the dye degrades as photo generated electrons and holes have a short lifetime [133].

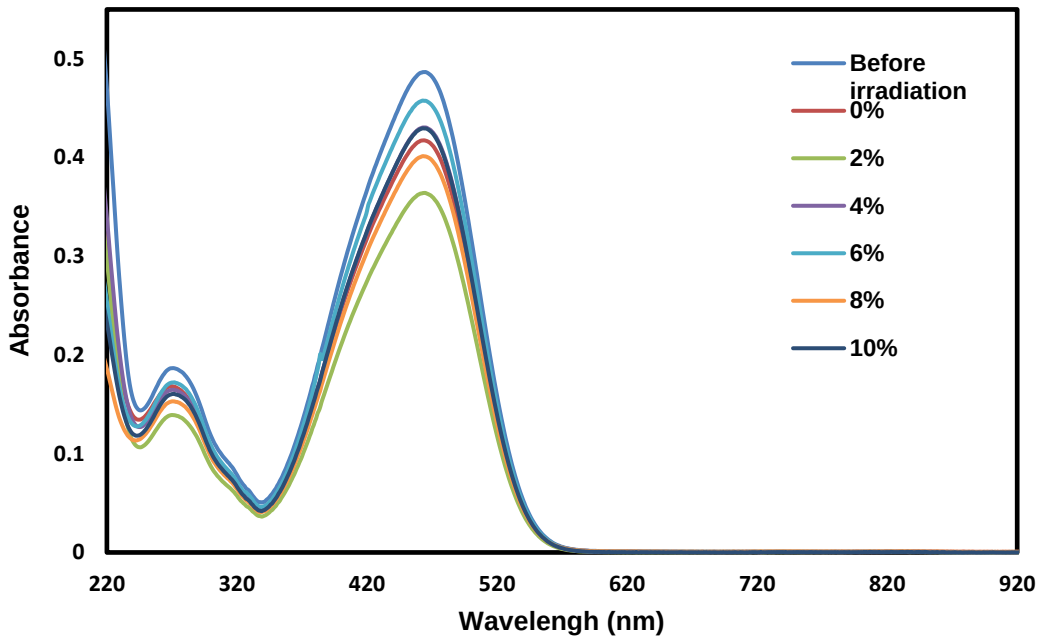

Figure 4.12 MO orange absorbance spectra before and after photocatalysis in the presence of undoped and Zn-doped TiO_2

The absorbance spectra of MO in the presence of Zn-doped TiO_2 thin films **(Figure 4.12)** shows the lowest absorbance of 0.3623 obtained by 2% Zn-doped followed by 8% with 0.3994. Although 10%, 4% and 6% showed a decrease in the absorbance compared to of the MO before irradiation, the undoped TiO_2 was able to degrade the dye more. The decrease in in absorbance is due to the fact that Zn does not provide shallow trap for photogenerated electron sand holes in order to avoid recombination before degradation [105].

Figure 4.13 shows the absorbance spectra of MO in the presence of Cu-doped TiO_2 thin films. These thin films showed a trend in absorbance with 2% Cu-doped having the highest absorbance but not the higher than the undoped TiO_2 thin films. The initial MO absorbance

of 0.4844, the value drops to 0.3448 with 6% Cu-doped TiO_2, indicating effective dye degradation under irradiation.

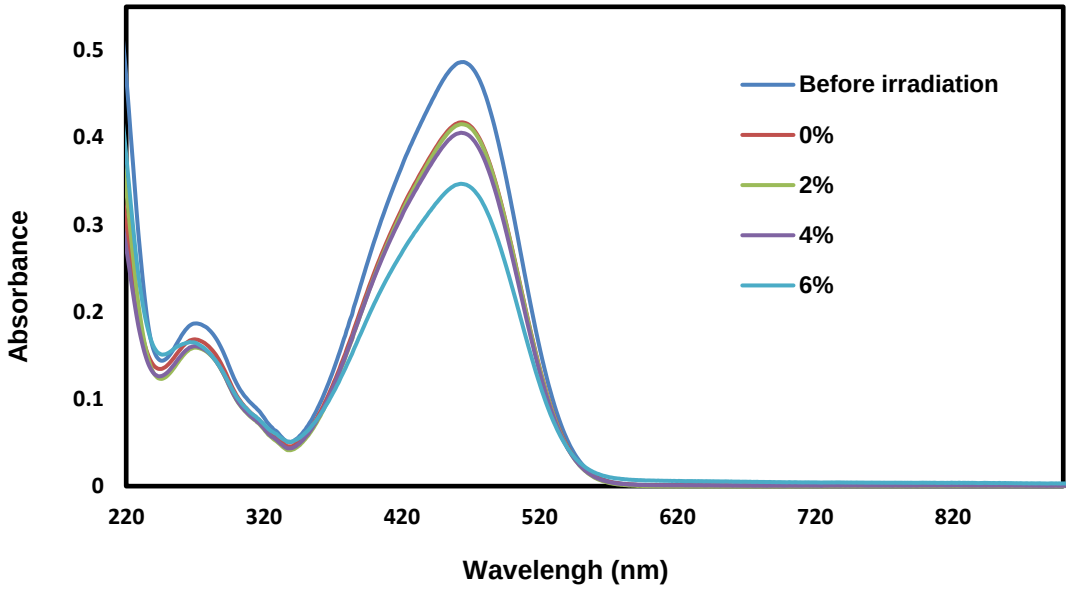

Figure 4.13 MO orange absorbance spectra before and after photocatalysis in the presence of undoped and Cu-doped TiO_2

This reduction in absorbance can be attributed to doping, which enhances charge separation and minimizes electron-hole recombination by modifying the electronic structure of TiO_2, shifting its absorption edge into the visible range. Consequently, higher doping levels improve photocatalytic efficiency by enabling more effective use of light energy for degradation [114].

The degradation effeciency of the undoped and doped TiO_2 thin films on the MO was calculated and plotted as a function of the doping concentration. **Figure 4.14** shows the degradation efficiency of Al-doped TiO_2 thin films on the MO where 8% demonstrated

the highest effeciency of about 14.62%, slightly increasing the degration of the undoped TiO_2 which had a degration effeciency of 14.275% while the 2% and 4% had no eefct on the degration effeciency and the 10% and 6% decreased the degration.

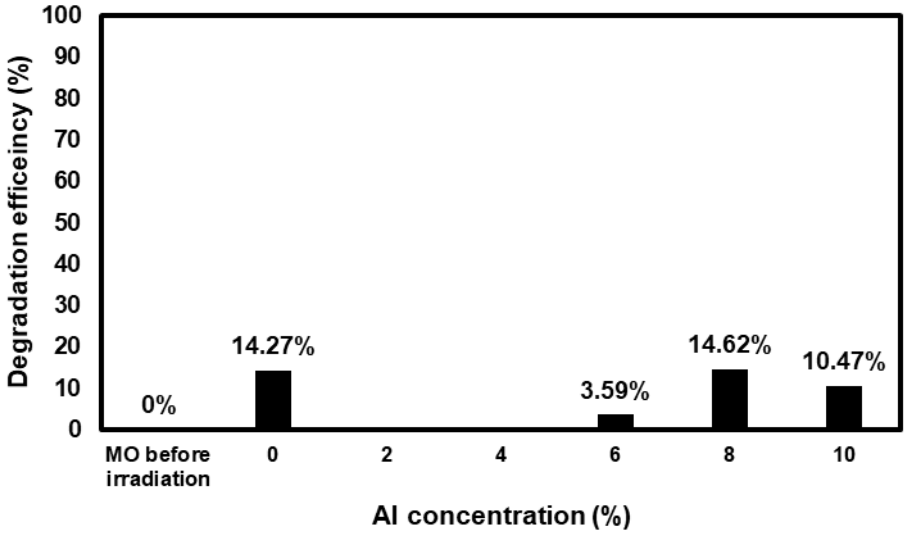

Figure 4.14 Degradation efficiency of undoped and Al-doped TiO_2 thin films on MO

The degradation efficiency of the Zn-doped TiO_2 **(Figure 4.15)** had an increase in the degradation efficiency increasing the degradation up to 25.215 by 2% and 17.55 by 8% Zn-doped TiO_2 thin films while 4%, 6% and 10% decreased the degradation of the undoped TiO_2.

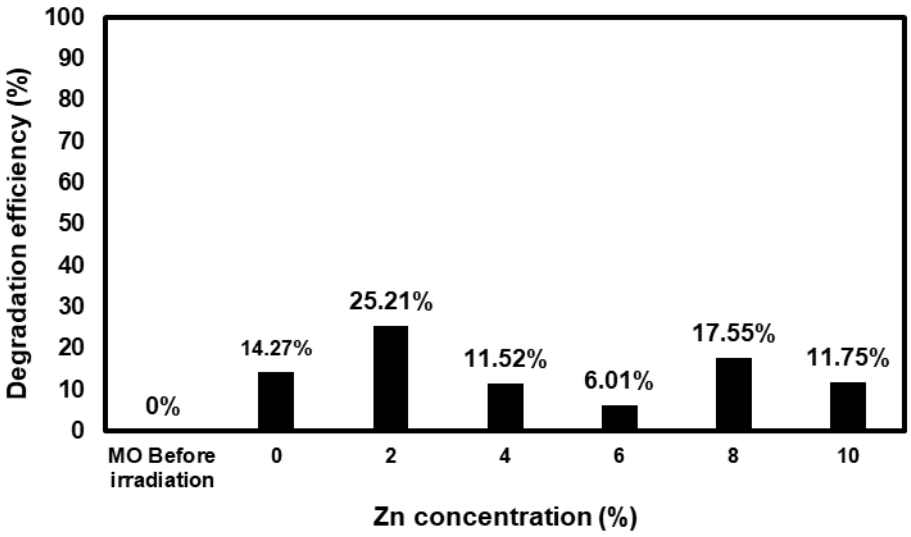

Figure 4.15 Degradation efficiency of undoped and Zn-doped TiO_2 thin films on MO

Cu-doped TiO_2 demonstrated the highest degradation efficiency of 28.82 by 6% Cu-doped thin films followed by 4% with 16.78% and 2% with 14.66% **(Figure 4.16).** The increase in degradation with increase in doping percentage of Cu is in accordance with literature where it has been noted that increasing Cu doping in TiO_2 creates more active sites on the catalyst surface, enhancing the formation of reactive species like electron-hole pairs and hydroxyl radicals which in return boosts the degradation efficiency since more radicals are available to break down contaminants [112].

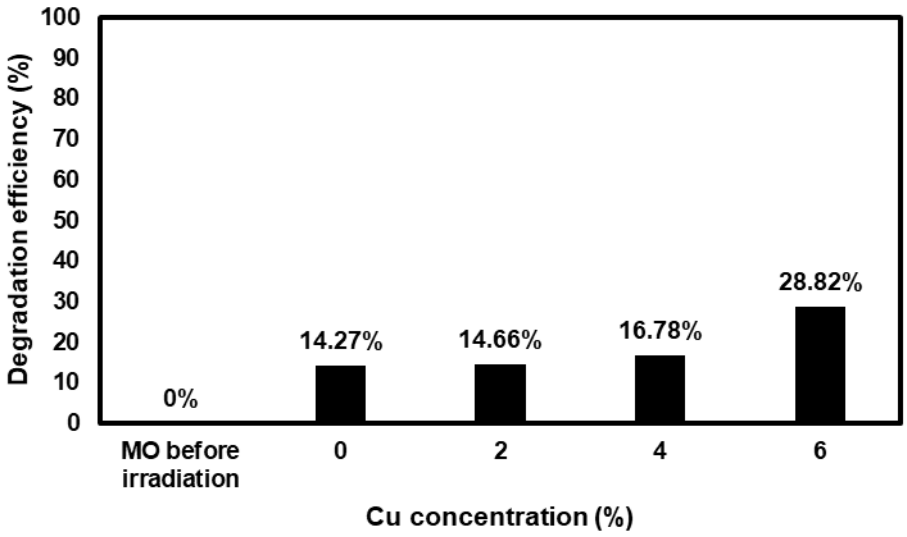

Figure 4.16 Degradation efficiency of undoped and Cu-doped TiO_2 thin films on MO

CHAPTER 5

Conclusion

This study evaluated and characterized TiO_2-based thin films, including Al, Zn and Cu doping, fabricated through the aqueous spray method, aiming to enhance their performance as anti-soiling coatings on solar cell cover glass. Results demonstrated that the doped TiO_2 films exhibited high optical transmittance, which is critical for maximizing solar cell efficiency, with anatase-phase TiO_2 confirmed by XRD patterns and no additional peaks for dopants. Additionally, the UV-vis and degradation studies indicated that doping influenced the optical absorption properties, with Al, Zn and Cu dopants showing varied effects based on concentration. The photocatalytic degradation of MO demonstrated that TiO_2 thin films, particularly at optimized doping levels, have the potential to reduce soiling effects by actively breaking down contaminants in the presence of irradiation. This work supports the application of TiO_2-based coatings as promising solutions to maintain solar panel efficiency, confirming that the aqueous spray method offers a reproducible and effective means for thin-film fabrication**.**

CHAPTER 6

Recommendations

Based on the findings, further research is recommended particularly focusing on optimizing doping concentrations, as incremental adjustments in doping levels may further improve transmittance and photocatalytic Additionally, conducting long-term stability tests under real-world environmental conditions, such as UV exposure and temperature fluctuations, would help assess the durability and practical applicability of the coatings. Moreover, investigating alternative doping elements or co-doping strategies may also enhance TiO_2's properties, as different ionic radii and electronic configurations could improve charge separation and absorption. Finally, applying the coatings in outdoor field tests on solar panels would provide valuable data on anti-soiling effectiveness and potential impacts on energy output.

REFERENCES

[1] Maka AOM, Alabid JM. Solar energy technology and its roles in sustainable development. *Clean Energy* 2022; 6: 476–483.

[2] Ahmed MG, Sharif AA. ENHANCING PHOTOVOLTAIC PANEL EFFICIENCY WITH AN IOT-ENABLED ROBOTIC CLEANING SYSTEM – A COMPREHENSIVE REVIEW. *Engineering and Technology Journal* 2023; 08: 2337–2338.

[3] Omar M, Arif A, Usman M, et al. Self-cleaning solution for solar panels. *SAIEE Africa Research Journal* 2023; 114: 58–66.

[4] Bhaduri S, Farkade M, Bajhal R, et al. Abrasion resistance of spray coated anti-soiling coatings during waterless cleaning of PV modules. *Mater Today Commun* 2023; 35: 106168.

[5] Borchers AM, Duke JM, Parsons GR. Does willingness to pay for green energy differ by source? *Energy Policy* 2007; 35: 3327–3334.

[6] Kumar V, Shrivastava RL, Untawale SP. Solar Energy: Review of Potential Green & Clean Energy for Coastal and Offshore Applications. *Aquat Procedia* 2015; 4: 473–480.

[7] Chaichan MT, Kazem HA. Experimental evaluation of dust composition impact on photovoltaic performance in Iraq. *Energy Sources, Part A: Recovery, Utilization, and Environmental Effects* 2020; 1–22.

[8] Maghami MR, Hizam H, Gomes C, et al. Power loss due to soiling on solar panel: A review. *Renewable and Sustainable Energy Reviews* 2016; 59: 1307–1316.

[9] Alshareef MJ. A Comprehensive Review of the Soiling Effects on PV Module Performance. *IEEE Access* 2023; 11: 134623–134651.

[10] Borah P, Micheli L, Sarmah N. Analysis of Soiling Loss in Photovoltaic Modules: A Review of the Impact of Atmospheric Parameters, Soil Properties, and Mitigation Approaches. *Sustainability* 2023; 15: 16669.

[11] Sayyah A, Horenstein MN, Mazumder MK. Energy yield loss caused by dust deposition on photovoltaic panels. *Solar Energy* 2014; 107: 576–604.

[12] Rahoma U, Hassan AH, HK E, et al. Effect of airborne dust concentration on the performance of PV modules. *J Astron Soc Egypt* 2005; 13: 24–38.

[13] Sayigh AAM, Al-jandal S, Ahmed H. Dust Effect on Solar Flat Surfaces Devices. *In Proceedings of the Workshop on the Physics of Non-Conventional Energy Sources and Materials Science for Energy* 1985; 353–367.

[14] HA. Kazem, MT Chaichan, AHA. Al-Waeli, K. Sopian. "A review of dust accumulation and cleaning methods for solar photovoltaic systems." Journal of Cleaner Production (2020): 123187.

[15] Said SAM, Hassan G, Walwil HM, et al. The effect of environmental factors and dust accumulation on photovoltaic modules and dust-accumulation mitigation strategies. *Renewable and Sustainable Energy Reviews* 2018; 82: 743–760.

[16] He G, Zhou C, Li Z. Review of Self-Cleaning Method for Solar Cell Array. *Procedia Eng* 2011; 16: 640–645.

[17] Kazem HA, Chaichan MT, Al-Waeli AH, et al. *Preprint-A review of dust accumulation and cleaning methods for solar photovoltaic systems*. 2020.

[18] Ayaz A, Ahmad H, Ahmad F, et al. Self-cleaning of glass surface to maximize the PV cell efficiency. In: *IOP Conference Series: Materials Science and Engineering*. IOP Publishing Ltd, 2020. Epub ahead of print 26 August 2020. DOI: 10.1088/1757-899X/899/1/012006.

[19] University of Namibia. Manual cleaning of solar cells at UNAM [photograph]. UNAM 2024.

[20] Chanchangi YN, Ghosh A, Sundaram S, et al. Dust and PV Performance in Nigeria: A review. *Renewable and Sustainable Energy Reviews* 2020; 121: 109704.

[21] Syafiq A, Pandey AK, Adzman NN, et al. Advances in approaches and methods for self-cleaning of solar photovoltaic panels. *Solar Energy* 2018; 162: 597–619.

[22] Jiang Y, Lu L, Lu H. A novel model to estimate the cleaning frequency for dirty solar photovoltaic (PV) modules in desert environment. *Solar Energy* 2016; 140: 236–240.

[23] Heydarabadi H, Abdolzadeh M, Lari K. Simulation of airflow and particle deposition settled over a tilted Photovoltaic module. *Energy* 2017; 139: 1016–1029.

[24] Xiong C, Zhang Y, Chen G, et al. Research on Dust Removal Strategies of Photovoltaic Panels in Ultra-high Altitude Photovoltaic Demonstration Base. In: *Journal of Physics: Conference Series*. Institute of Physics, 2023. Epub ahead of print 2023. DOI: 10.1088/1742-6596/2433/1/012025.

[25] Figgis B, Bermudez V, Lopez Garcia J. PV module vibration by robotic cleaning. *Solar Energy* 2023; 250: 168–172.

[26] Adak D, Bhattacharyya R, Barshilia HC. A state-of-the-art review on the multifunctional self-cleaning nanostructured coatings for PV panels, CSP mirrors

and related solar devices. *Renewable and Sustainable Energy Reviews*; 159. Epub ahead of print 1 May 2022. DOI: 10.1016/j.rser.2022.112145.

[27] Et al. J. Investigation of Superhydrophobic/Hydrophobic Materials Properties Using Electrospinning Technique. *Baghdad Science Journal* 2019; 16: 0632.

[28] Appasamy JS, Kurnia JC, Assadi MK. Synthesis and evaluation of nitrogen-doped titanium dioxide/single walled carbon nanotube-based hydrophilic self-cleaning coating layer for solar photovoltaic panel surface. *Solar Energy* 2020; 196: 80–91.

[29] Latthe S, Liu S, Terashima C, et al. Transparent, Adherent, and Photocatalytic SiO2-TiO2 Coatings on Polycarbonate for Self-Cleaning Applications. *Coatings* 2014; 4: 497–507.

[30] Magalhães P, Andrade L, Nunes O, et al. Titanium dioxide photocatalysis: Fundamentals and application on photoinactivation. *Reviews on Advanced Materials Science* 2017; 51: 91–129.

[31] Ambartsumov MG, Chapura OM, Tarala VA. Synthesis of titanium dioxide thin films via thermo- and plasma-enhanced atomic layer deposition. *Appl Surf Sci*; 672. Epub ahead of print 1 November 2024. DOI: 10.1016/j.apsusc.2024.160822.

[32] Magalhães P, Andrade L, Nunes OC, et al. *TITANIUM DIOXIDE PHOTOCATALYSIS: FUNDAMENTALS AND APPLICATION ON PHOTOINACTIVATION*. 2017.

[33] Oi LE, Choo M-Y, Lee HV, et al. Recent advances of titanium dioxide (TiO_2) for green organic synthesis. *RSC Adv* 2016; 6: 108741–108754.

[34] Hurum DC, Agrios AG, Gray KA, et al. Explaining the Enhanced Photocatalytic Activity of Degussa P25 Mixed-Phase TiO $_2$ Using EPR. *J Phys Chem B* 2003; 107: 4545–4549.

[35] Tripathi AK, Singh MK, Mathpal MC, et al. Study of structural transformation in TiO2 nanoparticles and its optical properties. *J Alloys Compd* 2013; 549: 114–120.

[36] Rehman S, Ullah R, Butt AM, et al. Strategies of making TiO2 and ZnO visible light active. *J Hazard Mater* 2009; 170: 560–569.

[37] Christy PD, Jothi NSN, Melikechi N, et al. Synthesis, structural and optical properties of well dispersed anatase TiO $_2$ nanoparticles by non-hydrothermal method. *Crystal Research and Technology* 2009; 44: 484–488.

[38] Auvinen S, Alatalo M, Haario H, et al. Size and Shape Dependence of the Electronic and Spectral Properties in TiO $_2$ Nanoparticles. *The Journal of Physical Chemistry C* 2011; 115: 8484–8493.

[39] Mo S-D, Ching WY. Electronic and optical properties of three phases of titanium dioxide: Rutile, anatase, and brookite. *Phys Rev B* 1995; 51: 13023–13032.

[40] Shaikh SF, Mane RS, Min BK, et al. D-sorbitol-induced phase control of TiO2 nanoparticles and its application for dye-sensitized solar cells. *Sci Rep* 2016; 6: 20103.

[41] FUJISHIMA A, ZHANG X, TRYK D. TiO2 photocatalysis and related surface phenomena. *Surf Sci Rep* 2008; 63: 515–582.

[42] Gupta SM, Tripathi M. A review of TiO2 nanoparticles. *Chinese Science Bulletin* 2011; 56: 1639–1657.

[43] Asahi R, Morikawa T, Ohwaki T, et al. Visible-Light Photocatalysis in Nitrogen-Doped Titanium Oxides. *Science (1979)* 2001; 293: 269–271.

[44] Akakuru OU, Iqbal ZM, Wu A. TiO2 Nanoparticles: Properties and applications. In: *TiO2 Nanoparticles*. Wiley, 2020, pp. 1–66.

[45] Maness P-C, Smolinski S, Blake DM, et al. Bactericidal Activity of Photocatalytic TiO $_2$ Reaction: toward an Understanding of Its Killing Mechanism. *Appl Environ Microbiol* 1999; 65: 4094–4098.

[46] Jesline A, John NP, Narayanan PM, et al. Antimicrobial activity of zinc and titanium dioxide nanoparticles against biofilm-producing methicillin-resistant Staphylococcus aureus. *Appl Nanosci* 2015; 5: 157–162.

[47] Chorianopoulos NG, Tsoukleris DS, Panagou EZ, et al. Use of titanium dioxide (TiO2) photocatalysts as alternative means for Listeria monocytogenes biofilm disinfection in food processing. *Food Microbiol* 2011; 28: 164–170.

[48] Huang Y-Y, Choi H, Kushida Y, et al. Broad-Spectrum Antimicrobial Effects of Photocatalysis Using Titanium Dioxide Nanoparticles Are Strongly Potentiated by Addition of Potassium Iodide. *Antimicrob Agents Chemother* 2016; 60: 5445–5453.

[49] Watts RJ, Kong S, Orr MP, et al. Photocatalytic inactivation of coliform bacteria and viruses in secondary wastewater effluent. *Water Res* 1995; 29: 95–100.

[50] Bai Y, Mora-Seró I, De Angelis F, et al. Titanium Dioxide Nanomaterials for Photovoltaic Applications. *Chem Rev* 2014; 114: 10095–10130.

[51] Carbajo J, Tolosana-Moranchel A, Casas JA, et al. Analysis of photoefficiency in TiO2 aqueous suspensions: Effect of titania hydrodynamic particle size and catalyst loading on their optical properties. *Appl Catal B* 2018; 221: 1–8.

[52] Chen X, Mao SS. Titanium Dioxide Nanomaterials: Synthesis, Properties, Modifications, and Applications. *Chem Rev* 2007; 107: 2891–2959.

[53] Rehman FU, Zhao C, Jiang H, et al. Biomedical applications of nano-titania in theranostics and photodynamic therapy. *Biomater Sci* 2016; 4: 40–54.

[54] Baraton M-I, Merhari L. Surface chemistry of TiO2 nanoparticles: influence on electrical and gas sensing properties. *J Eur Ceram Soc* 2004; 24: 1399–1404.

[55] Liu X, Chen G, Keller AA, et al. Effects of dominant material properties on the stability and transport of TiO_2 nanoparticles and carbon nanotubes in aquatic environments: from synthesis to fate. *Environ Sci: Processes Impacts* 2013; 15: 169–189.

[56] Kavan L. Electrochemistry of titanium dioxide: some aspects and highlights. *The Chemical Record* 2012; 12: 131–142.

[57] Yang Z, Choi D, Kerisit S, et al. Nanostructures and lithium electrochemical reactivity of lithium titanites and titanium oxides: A review. *J Power Sources* 2009; 192: 588–598.

[58] Li X, Zhang Y, Li T, et al. Graphene nanoscrolls encapsulated TiO2 (B) nanowires for lithium storage. *J Power Sources* 2014; 268: 372–378.

[59] Winter M, Brodd RJ. What Are Batteries, Fuel Cells, and Supercapacitors? *Chem Rev* 2004; 104: 4245–4270.

[60] Whittingham MS, Savinell RF, Zawodzinski T. Introduction: Batteries and Fuel Cells. *Chem Rev* 2004; 104: 4243–4244.

[61] Paracchino A, Laporte V, Sivula K, et al. Highly active oxide photocathode for photoelectrochemical water reduction. *Nat Mater* 2011; 10: 456–461.

[62] FUJISHIMA A, HONDA K. Electrochemical Photolysis of Water at a Semiconductor Electrode. *Nature* 1972; 238: 37–38.

[63] Maeda K, Xiong A, Yoshinaga T, et al. Photocatalytic Overall Water Splitting Promoted by Two Different Cocatalysts for Hydrogen and Oxygen Evolution under Visible Light. *Angewandte Chemie International Edition* 2010; 49: 4096–4099.

[64] Kudo A, Miseki Y. Heterogeneous photocatalyst materials for water splitting. *Chem Soc Rev* 2009; 38: 253–278.

[65] Liu S, Yu J, Jaroniec M. Anatase TiO_2 with Dominant High-Energy {001} Facets: Synthesis, Properties, and Applications. *Chemistry of Materials* 2011; 23: 4085–4093.

[66] Yu J, Qi L, Jaroniec M. Hydrogen Production by Photocatalytic Water Splitting over Pt/TiO_2 Nanosheets with Exposed (001) Facets. *The Journal of Physical Chemistry C* 2010; 114: 13118–13125.

[67] Ksibi M, Rossignol S, Tatibouët JM, et al. Synthesis and solid characterization of nitrogen and sulfur-doped TiO2 photocatalysts active under near visible light. *Mater Lett* 2008; 62: 4204–4206.

[68] Murdoch M, Waterhouse GIN, Nadeem MA, et al. The effect of gold loading and particle size on photocatalytic hydrogen production from ethanol over Au/TiO2 nanoparticles. *Nat Chem* 2011; 3: 489–492.

[69] Zuo F, Wang L, Wu T, et al. Self-Doped Ti^{3+} Enhanced Photocatalyst for Hydrogen Production under Visible Light. *J Am Chem Soc* 2010; 132: 11856–11857.

[70] Justicia I, Ordejón P, Canto G, et al. Designed Self-Doped Titanium Oxide Thin Films for Efficient Visible-Light Photocatalysis. *Advanced Materials* 2002; 14: 1399–1402.

[71] Thompson TL, Yates JT. Surface Science Studies of the Photoactivation of TiO_2 New Photochemical Processes. *Chem Rev* 2006; 106: 4428–4453.

[72] Kim HG, Hwang DW, Lee JS. An Undoped, Single-Phase Oxide Photocatalyst Working under Visible Light. *J Am Chem Soc* 2004; 126: 8912–8913.

[73] Park JH, Kim S, Bard AJ. Novel Carbon-Doped TiO_2 Nanotube Arrays with High Aspect Ratios for Efficient Solar Water Splitting. *Nano Lett* 2006; 6: 24–28.

[74] Mou J, Lin T, Huang F, et al. Black titania-based theranostic nanoplatform for single NIR laser induced dual-modal imaging-guided PTT/PDT. *Biomaterials* 2016; 84: 13–24.

[75] Carbajo J, Bahamonde A, Faraldos M. Photocatalyst performance in wastewater treatment applications: Towards the role of TiO2 properties. *Molecular Catalysis* 2017; 434: 167–174.

[76] Nasikhudin, Diantoro M, Kusumaatmaja A, et al. Study on Photocatalytic Properties of TiO_2 Nanoparticle in various pH condition. *J Phys Conf Ser* 2018; 1011: 012069.

[77] Behnajady MA, Eskandarloo H, Modirshahla N, et al. Investigation of the effect of sol–gel synthesis variables on structural and photocatalytic properties of TiO2 nanoparticles. *Desalination* 2011; 278: 10–17.

[78] Matsuyama H, Teramoto M, Matsui K, et al. Preparation of poly(acrylic acid)/poly(vinyl alcohol) membrane for the facilitated transport of CO_2. *J Appl Polym Sci* 2001; 81: 936–942.

[79] Yang M-Q, Zhang N, Xu Y-J. Synthesis of Fullerene–, Carbon Nanotube–, and Graphene–TiO_2 Nanocomposite Photocatalysts for Selective Oxidation: A Comparative Study. *ACS Appl Mater Interfaces* 2013; 5: 1156–1164.

[80] Meng L-Y, Park S-J. Influence of carbon nanofibers on electrochemical properties of carbon nanofibers/glass fibers composites. *Current Applied Physics* 2013; 13: 640–644.

[81] De Volder MFL, Tawfick SH, Baughman RH, et al. Carbon Nanotubes: Present and Future Commercial Applications. *Science (1979)* 2013; 339: 535–539.

[82] Gázquez MJ, Bolívar JP, Garcia-Tenorio R, et al. A Review of the Production Cycle of Titanium Dioxide Pigment. *Materials Sciences and Applications* 2014; 05: 441–458.

[83] Braun JH, Baidins A, Marganski RE. TiO2 pigment technology: a review. *Prog Org Coat* 1992; 20: 105–138.

[84] Wu X. Applications of Titanium Dioxide Materials. In: *Titanium Dioxide - Advances and Applications*. IntechOpen, 2022. Epub ahead of print 2 March 2022. DOI: 10.5772/intechopen.99255.

[85] Afzal A, Habib A, Ulhasan I, et al. Antireflective Self-Cleaning TiO2 Coatings for Solar Energy Harvesting Applications. *Frontiers in Materials*; 8. Epub ahead of print 7 June 2021. DOI: 10.3389/fmats.2021.687059.

[86] Isaifan RJ, Samara A, Suwaileh W, et al. Improved Self-cleaning Properties of an Efficient and Easy to Scale up TiO2 Thin Films Prepared by Adsorptive Self-Assembly. *Sci Rep*; 7. Epub ahead of print 1 December 2017. DOI: 10.1038/s41598-017-07826-0.

[87] Haider AJ, Jameel ZN, Taha SY. *Synthesis and Characterization of TiO 2 Nanoparticles via Sol-Gel Method by Pulse Laser Ablation*.

[88] Wu X. Applications of Titanium Dioxide Materials. In: *Titanium Dioxide - Advances and Applications*. IntechOpen, 2022. Epub ahead of print 2 March 2022. DOI: 10.5772/intechopen.99255.

[89] Linsebigler AL, Lu G, Yates JT. Photocatalysis on TiO2 Surfaces: Principles, Mechanisms, and Selected Results. *Chem Rev* 1995; 95: 735–758.

[90] Al-Rasheed R, Arabia S. Water treatment by heterogenous photocatalysis: An overview 1, https://api.semanticscholar.org/CorpusID:103717634 (2005).

[91] Kotani Y, Matoda T, Matsuda A, et al. Anatase nanocrystaldispersed thin films via sol–gel process with hot water treatment: effects of poly(ethylene glycol) addition on photocatalytic activities of the films. *J Mater Chem* 2001; 11: 2045–2048.

[92] Mills A, Le Hunte S. An overview of semiconductor photocatalysis. *J Photochem Photobiol A Chem* 1997; 108: 1–35.

[93] Komaraiah D, P.Madhukar, Vijayakumar Y, et al. Photocatalytic degradation study of methylene blue by brookite TiO2 thin film under visible light irradiation. *Mater Today Proc* 2016; 3: 3770–3778.

[94] Trabelsi H, Khadhraoui M, Hentati O, et al. Titanium dioxide mediated photo-degradation of methyl orange by ultraviolet light. *Toxicol Environ Chem* 2013; 95: 543–558.

[95] Park J-J, Kim D-Y, Latthe SS, et al. Thermally Induced Superhydrophilicity in TiO 2 Films Prepared by Supersonic Aerosol Deposition. *ACS Appl Mater Interfaces* 2013; 5: 6155–6160.

[96] Kaveh R, Alijani H, Falletta E, et al. Advancements in superhydrophilic titanium dioxide/graphene oxide composites coatings for self-cleaning applications on glass substrates: A comprehensive review. *Prog Org Coat* 2024; 190: 108347.

[97] Banerjee S, Dionysiou DD, Pillai SC. Self-cleaning applications of TiO2 by photo-induced hydrophilicity and photocatalysis. *Appl Catal B* 2015; 176–177: 396–428.

[98] Daoud WA, Tung WS. Self-Cleaning Fibers via Nanotechnology - A Virtual Reality. In: *2008 8th IEEE Conference on Nanotechnology*. IEEE, 2008, pp. 1–2.

[99] Lukong VT, Mouchou RT, Enebe GC, et al. Deposition and characterization of self-cleaning TiO2 thin films for photovoltaic application. *Mater Today Proc* 2022; 62: S63–S72.

[100] Lopes D, Conceição R, Silva HG, et al. Anti-soiling coating performance assessment on the reduction of soiling effect in second-surface solar mirror. *Solar Energy* 2019; 194: 478–484.

[101] Kaur T, Sraw A, Toor AP, et al. Utilization of solar energy for the degradation of carbendazim and propiconazole by Fe doped TiO2. *Solar Energy* 2016; 125: 65–76.

[102] Appasamy JS, Kurnia JC, Assadi MK. Synthesis and evaluation of nitrogen-doped titanium dioxide/single walled carbon nanotube-based hydrophilic self-cleaning coating layer for solar photovoltaic panel surface. *Solar Energy* 2020; 196: 80–91.

[103] Motiur Mazumder MR, Akteruzzaman M, Islam R. *Doping in TiO 2 to improve solar cell efficiency: A Comprehensive Review*.

[104] Pérez-Nicolás M, Navarro-Blasco I, Fernández JM, et al. Atmospheric NOx removal: Study of cement mortars with iron- and vanadium-doped TiO2 as visible light–sensitive photocatalysts. *Constr Build Mater* 2017; 149: 257–271.

[105] Zhang W, Zhu S, Li Y, et al. Photocatalytic Zn-doped TiO2 films prepared by DC reactive magnetron sputtering. *Vacuum* 2007; 82: 328–335.

[106] Al-Mosawi BTSh, Al-Hashimi MK, Abdulameer AF. Aluminum-Doped Titanium Dioxide Thin Films: A Study of Different Concentrations on Poly(3-hexylthiophene): PhenylC61-Butyric Acid Metheyester-Based Organic Solar Cells. *J Comput Theor Nanosci* 2020; 17: 4849–4854.

[107] Pathak SK, Abate A, Ruckdeschel P, et al. Performance and Stability Enhancement of Dye-Sensitized and Perovskite Solar Cells by Al Doping of TiO $_2$. *Adv Funct Mater* 2014; 24: 6046–6055.

[108] Anjum F, Samir Ullah M, Podder J, et al. Electrical and Optical Properties of Zinc doped Titanium dioxide Thin Films. In: *2018 International Conference on Innovations in Science, Engineering and Technology (ICISET)*. IEEE, 2018, pp. 138–142.

[109] JAIN A, VAYA D. PHOTOCATALYTIC ACTIVITY OF TiO2 NANOMATERIAL. *Journal of the Chilean Chemical Society* 2017; 62: 3683–3690.

[110] Yang XJ, Wang S, Sun HM, et al. Preparation and photocatalytic performance of Cu-doped TiO2 nanoparticles. *Transactions of Nonferrous Metals Society of China (English Edition)* 2015; 25: 504–509.

[111] Sokoidanto H, Taufik A, Saleh R. Structural and optical study of Cu-doped TiO_2 nanoparticles synthesized by co-precipitation method. *J Phys Conf Ser* 2020; 1442: 012008.

[112] Ahmadiasl R, Moussavi G, Shekoohiyan S, et al. Synthesis of Cu-Doped TiO2 Nanocatalyst for the Enhanced Photocatalytic Degradation and Mineralization of Gabapentin under UVA/LED Irradiation: Characterization and Photocatalytic Activity. *Catalysts*; 12. Epub ahead of print 1 November 2022. DOI: 10.3390/catal12111310.

[113] Pava-Gómez B, Vargas-Ramírez X, Díaz-Uribe C. Physicochemical study of adsorption and photodegradation processes of methylene blue on copper-doped TiO2 films. *J Photochem Photobiol A Chem* 2018; 360: 13–25.

[114] Bensouici F, Bououdina M, Dakhel AA, et al. Optical, structural and photocatalysis properties of Cu-doped TiO 2 thin films. *Appl Surf Sci* 2017; 395: 110–116.

[115] Halin DSC, Abidin ASZ, Azani A, et al. Synthesis of Zn/TiO_2 Thin Films for Self-Cleaning Applications. *Acta Phys Pol A* 2022; 142: 164–167.

[116] Park S, Yoon Y, Lee S, et al. Thermoinduced and Photoinduced Sustainable Hydrophilic Surface of Sputtered-TiO2 Thin Film. *Coatings* 2021; 11: 1360.

[117] Geremew T. Thin Film Deposition and Characterization Techniques. *Journal of 3D Printing and Applications* 2022; 1: 1–24.

[118] Chaudhari MN. Thin film Deposition Methods: A Critical Review. *Int J Res Appl Sci Eng Technol* 2021; 9: 5215–5232.

[119] Hishimone PN, Nagai H, Sato M. *Methods of Fabricating Thin Films for Energy Materials and Devices*, www.intechopen.com.

[120] Nimalan T, Begam MR. Physical and Chemical Methods: A Review on the Analysis of Deposition Parameters of Thin Film Preparation Methods. *International Journal of Thin Film Science and Technology* 2024; 13: 59–66.

[121] Oluwatosin Abegunde O, Titilayo Akinlabi E, Philip Oladijo O, et al. Overview of thin film deposition techniques. *AIMS Mater Sci* 2019; 6: 174–199.

[122] Jilani A, Abdel-wahab MS, Hammad AH. Advance Deposition Techniques for Thin Film and Coating. In: *Modern Technologies for Creating the Thin-film Systems and Coatings*. InTech, 2017. Epub ahead of print 8 March 2017. DOI: 10.5772/65702.

[123] Hishimone PN, Nagai H, Morita M, et al. Highly-conductive and well-adhered Cu thin film fabricated on quartz glass by heat treatment of a precursor film obtained via spray-coating of an aqueous solution involving Cu(II) complexes. *Coatings*; 8. Epub ahead of print 2018. DOI: 10.3390/COATINGS8100352.

[124] Kadhingula Tunelago, Philipus N. Hishimone, Likius S. Daniel. *Fabrication of TiO2/Ag Composite Thin Films from Aqueous Precursors Involving Ti4+ and Ag+, via the Spray-Coating Method*. University of Namibia, 2019.

[125] Mutenda GK, Hishimone PN. *Fabrication and characterization of Al-doped TiO2 thin films by the spray–coating method using aqueous precursors involving Ti4+ and Al3+ complexes.* University of Namibia, 2021.

[126] Giolando DM. Nano-crystals of titanium dioxide in aluminum oxide: A transparent self-cleaning coating applicable to solar energy. *Solar Energy* 2013; 97: 195–199.

[127] Rhine WE, Hallock RB, Davis WM, et al. *Control of Ceramic Powder Composition by Precipitation Techniques. In Ceramic Powder Science 111 Ceramic Transactions*. American Ceramic Society: Columbus, 1992.

[128] Nguyen TMH, Bark CW. Synthesis of Cobalt-Doped TiO_2 Based on Metal–Organic Frameworks as an Effective Electron Transport Material in Perovskite Solar Cells. *ACS Omega* 2020; 5: 2280–2286.

[129] Sassi S, Bouich A, Hajjaji A, et al. Cu-Doped TiO2 Thin Films by Spin Coating: Investigation of Structural and Optical Properties. *Inorganics (Basel)*; 12. Epub ahead of print 1 July 2024. DOI: 10.3390/inorganics12070188.

[130] Hashim F, Ismail K, Supee A, et al. *Aluminum Doped Titanium Dioxide Thin Film for Perovskite Electron Transport Layer*. 2022.

[131] Kriel FH, Priest C. Influence of Sample Volume and Solvent Evaporation on Absorbance Spectroscopy in a Microfluidic “Pillar-Cuvette”. *Analytical Sciences* 2016; 32: 103–108.

[132] Beydaghdari M, Asgari M, Saboor FH. Metal organic frameworks for photocatalytic water treatment. In: Alireza Bazargan (ed) *Photocatalytic Water and Wastewater Treatment*. IWA Publishing, 2022, pp. 37–72.

[133] Khlyustova A, Sirotkin N, Kusova T, et al. Doped TiO_2: the effect of doping elements on photocatalytic activity. *Mater Adv* 2020; 1: 1193–1201.

Appendix I: Ethical clearance

UNAM
UNIVERSITY OF NAMIBIA

ETHICAL CLEARANCE CERTIFICATE

Ethical Clearance Reference Number: SOS-0241 **Date: 20 SEPTEMBER 2024**

This Ethical Clearance Certificate is issued by the University of Namibia Ethics Committee (REC) in accordance with the University of Namibia's Research Ethics Policy and Guidelines. Ethical approval is given in respect of undertakings contained in the Research Project outlined below. This Certificate is issued on the recommendations of the ethical evaluation done by the ethics committee.

Title of Project: EVALUATION OF TiO2-BASED THIN FILMS FABRICATED VIA THE AQUEOUS SPRAY METHOD FOR APPLICATIONS AS ANTI-SOILING COATINGS ON SOLAR CELL COVER GLASS

Student: KLAUDIA MWATILE

Student Number: 218201499

Supervisor(s): DR. PHILIPUS HISHIMONE

Centre for Research Services

Take note of the following:

1. Any significant changes in the conditions or undertakings outlined in the approved Proposal must be communicated to the ethics committee. An application to make amendments may be necessary.
2. Any breaches of ethical undertakings or practices that have an impact on ethical conduct of the research must be reported to the ethics committee.
3. The Principal Researcher must report issues of ethical compliance to the ethics committee (through the Chairperson) at the end of the Project or as may be requested by the ethics committee.
4. The ethics committee retains the right to:

i) Withdraw or amend this Ethical Clearance if any unethical practices (as outlined in the Research Ethics Policy) have been detected or suspected,

ii) Request for an ethical compliance report at any point during the course of the research.

The ethics committee wishes you the best in your research.

Prof. Ezekeil Gwinyai Kwembeya (Chairperson Ethics Committee)

Prof. Davis Mumbengegwi (Head, Multidisciplinary Research

Appendix II: Research permission letter

CENTRE FOR RESEARCH SERVICES
Office of the Pro-Vice Chancellor: Research, Innovation & Development
University of Namibia, Private Bag 13301, Windhoek, Namibia
340 Mandume Ndemufayo Avenue, Pioneers Park, Office F223 - Fblock, Second Floor
☎ +264 61 206 4673; E-mail:kmbulu@unam.na; URL.: http//www.unam.edu.na

UNAM
UNIVERSITY OF NAMIBIA

RESEARCH PERMISSION LETTER

Date: 28/10/2024

Student Name: KLAUDIA MWATILE

Student Number: 218201499

Programme: Master of science in Renewable energy

Approved Research Title: EVALUATION OF TiO2-BASED THIN FILMS FABRICATED VIA THE AQUEOUS SPRAY METHOD FOR APPLICATIONS AS ANTI SOILING COATINGS ON SOLAR CELL COVER GLASS

TO WHOM IT MAY CONCERN:

I hereby confirm that the above-mentioned student is registered at the University of Namibia for the programme indicated. The proposed study met all the requirements as stipulated in the University guidelines and has been approved by the relevant committees.

The proposal adheres to ethical principles as per attached Ethical Clearance Certificate. Permission is hereby granted to carry out the research as described in the approved proposal.

Best Regards

Dr. AEE Shikongo
Head: Postgraduate Research Support Services
Tel: +264 61 206 3129
E-mail: aeshikongo@unam.na

CENTRE FOR RESEARCH SERVICES
Office of the Director
2024 -10- 28
University of Namibia
UNAM